Direct observation of the Migdal effect induced by neutron bombardment

米格达尔(Migdal)效应的直接观测

Nature **649**, 580 (2026)

刘　倩　(代表 **MARVEL** 合作组团队)

Migd**A**l p**R**ocess **V**alidation by n**E**utrua**L** scattering (中性散射中的Migdal过程验证)

中国科学院大学

2026 SYSU International Summer Program

Visible matter is just the tip of the iceberg

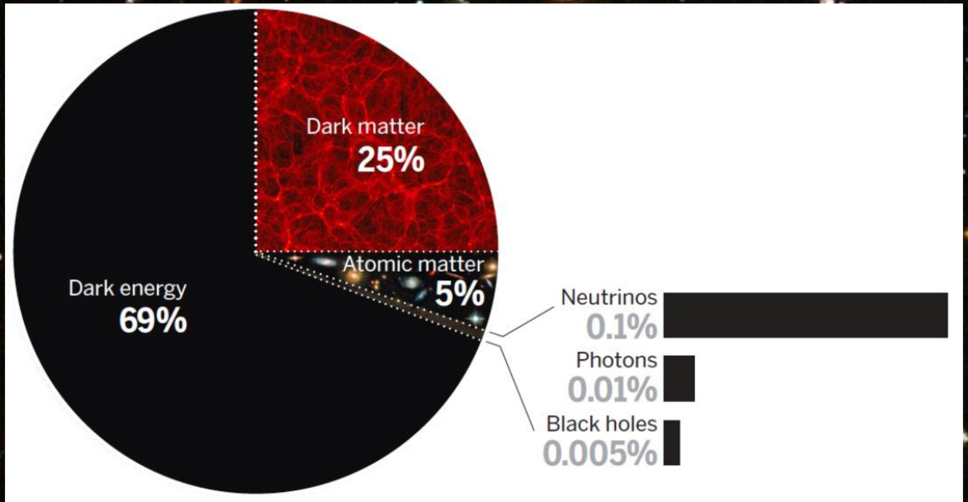

- Dark matter makes up most of the mass in galaxies and galaxy clusters.
- Current evidence comes solely from gravitational interaction.

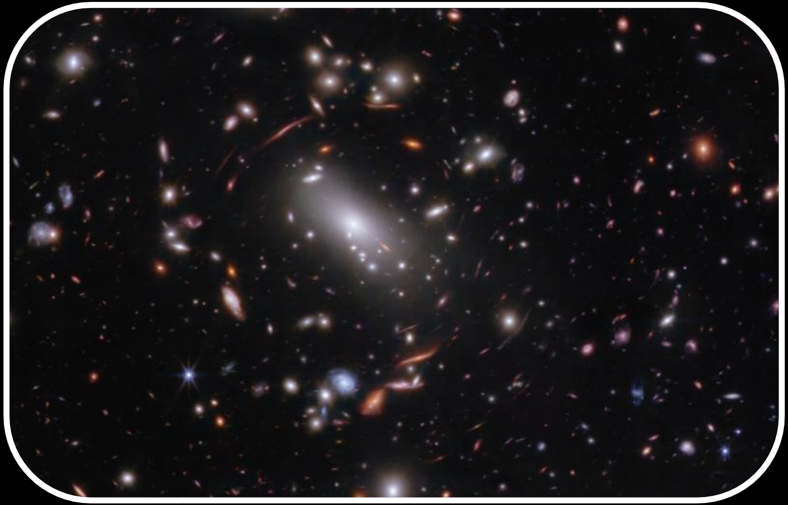

Gravitational Lens

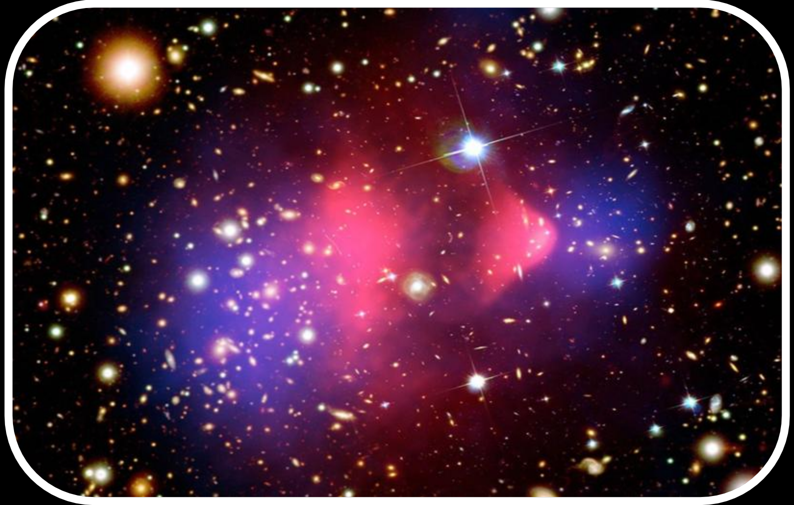

Galaxy mergers

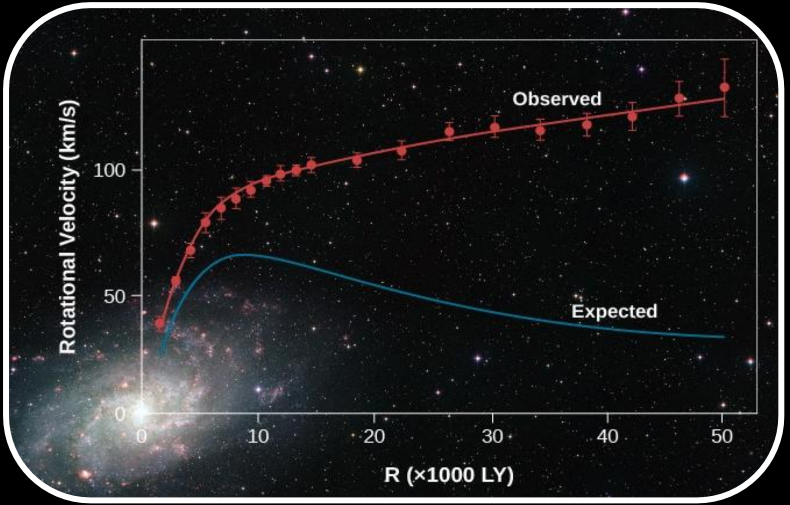

Galactic rotation curve

银河系周围的暗物质

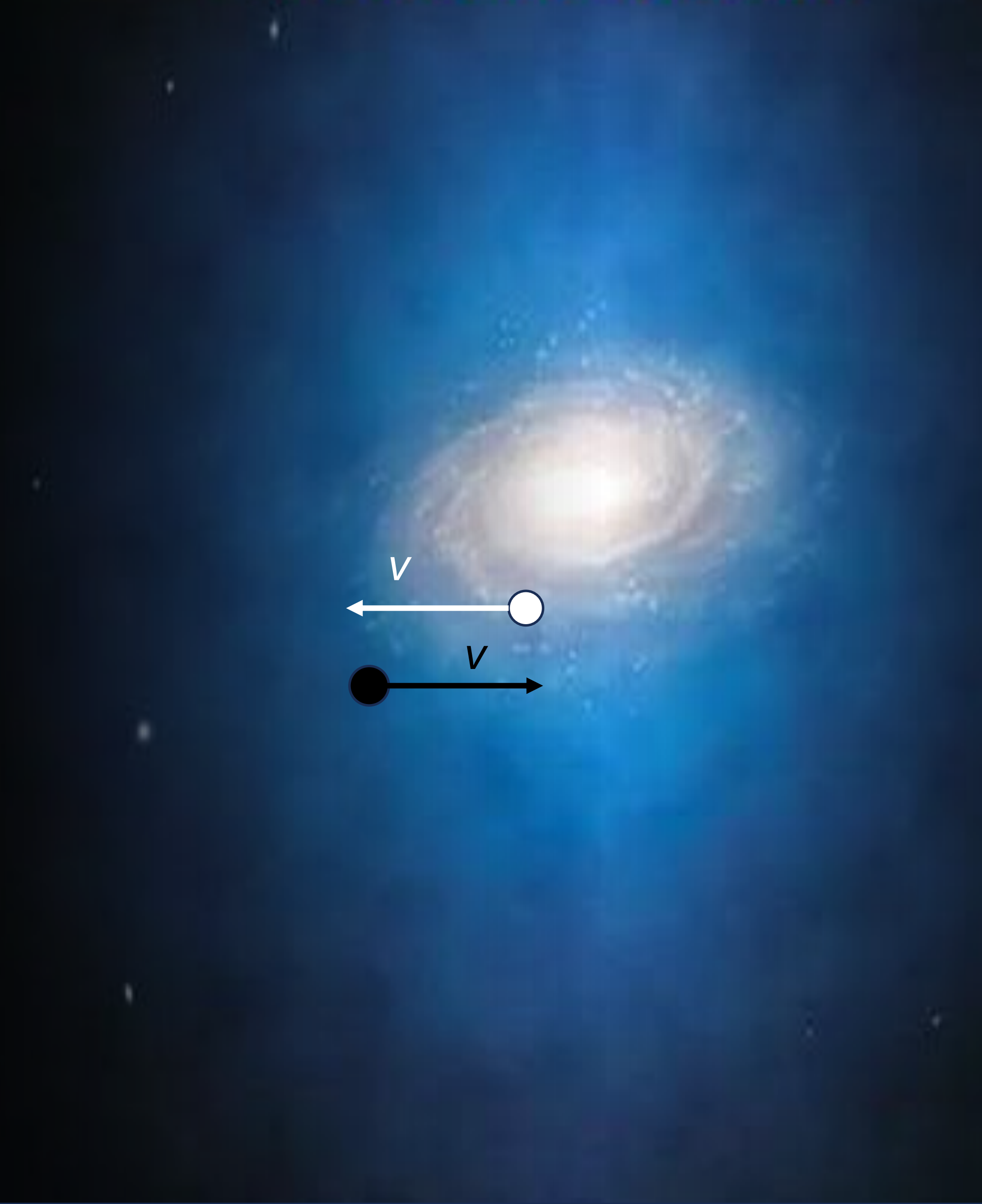

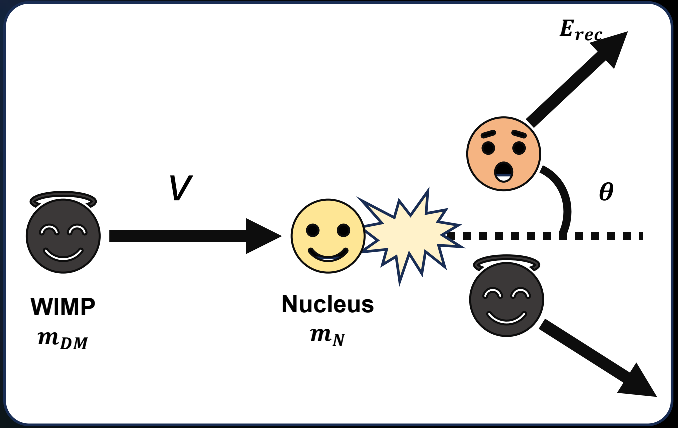

WIMP

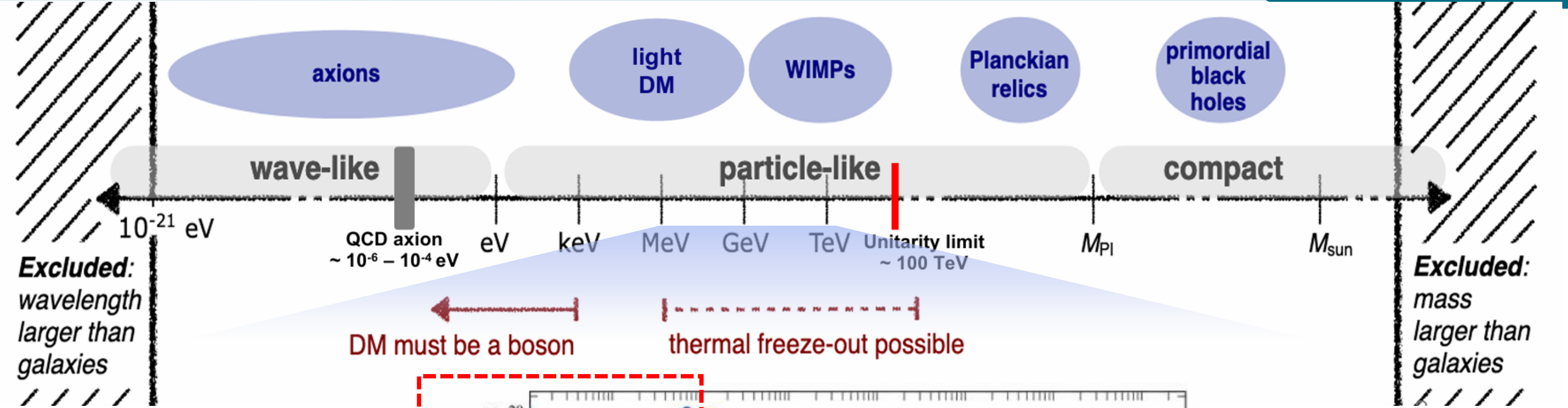
axions
light DM
WIMPs
Planckian relics
primordial black holes
wave-like
particle-like
compact
10^-21 eV
QCD axion
~ 10^-6 – 10^-4 eV
eV
keV
MeV
GeV
TeV
Unitarity limit
~ 100 TeV
M_Pl
M_sun
Excluded: wavelength larger than galaxies
Excluded: mass larger than galaxies
DM must be a boson
thermal freeze-out possible

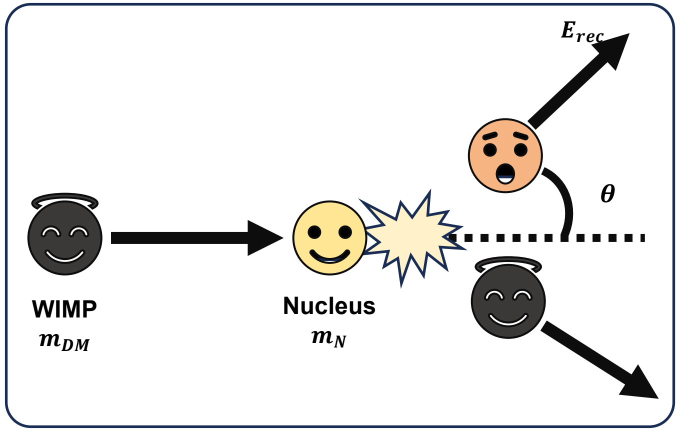
E_rec
θ
WIMP
m_DM
Nucleus
m_N

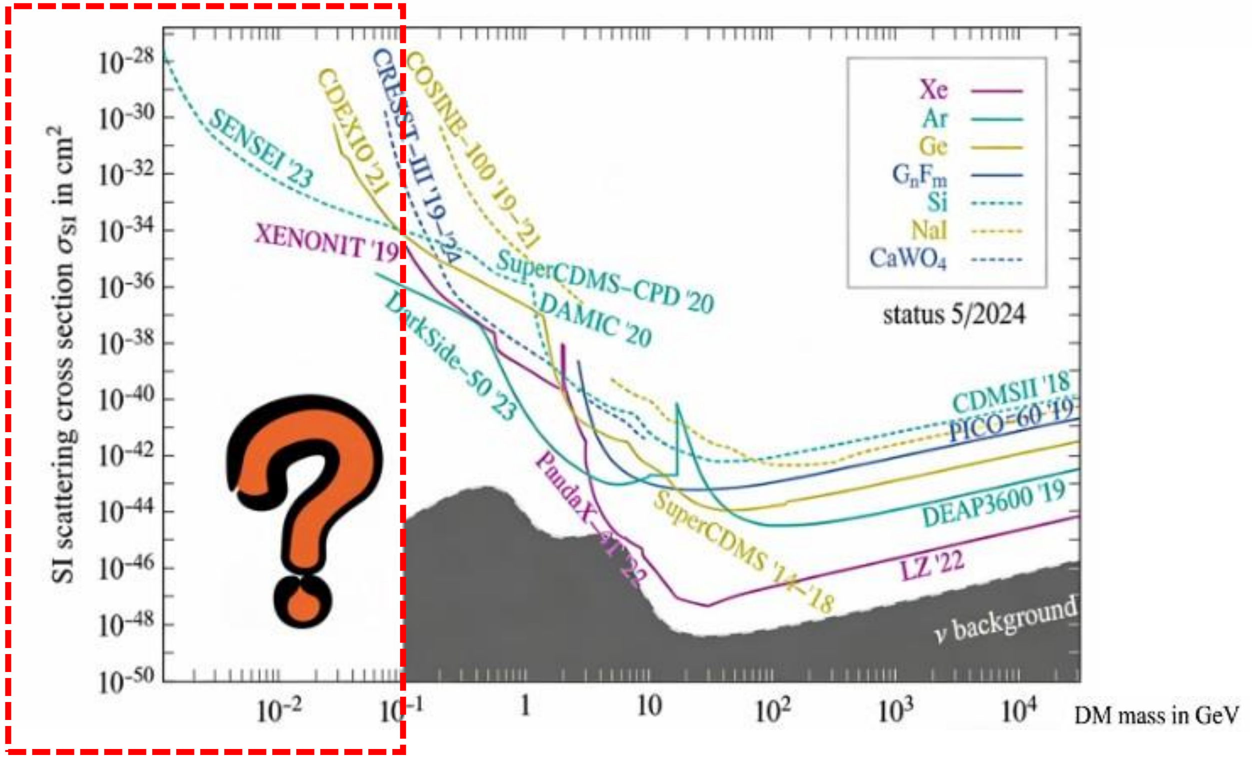
SI scattering cross section σ_SI in cm²
DM mass in GeV
SENSEI '23
CDEX10 '21
CRESST-III '19-'24
COSINE-100 '19-'21
XENON1T '19
SuperCDMS-CPD '20
DAMIC '20
DarkSide-50 '23
PandaX-4T '22
SuperCDMS '14-'18
CDMSII '18
PICO-60 '19
DEAP3600 '19
LZ '22
ν background
Xe
Ar
Ge
GnFm
Si
NaI
CaWO4
status 5/2024

从卢瑟福散射实验说起

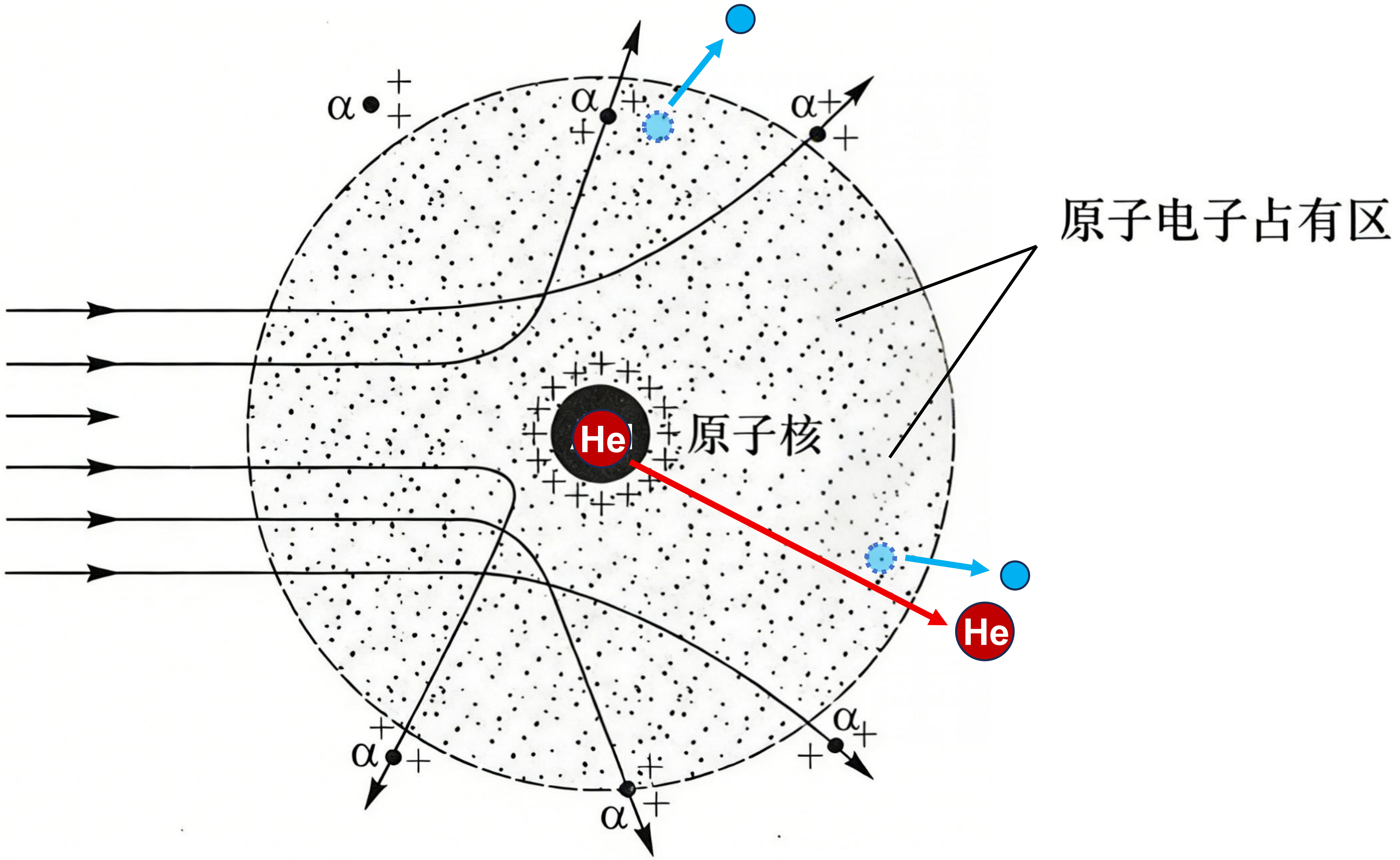

Dark matter experiments

WIMP dark matter searches, PIC-2025

- Dark matter scattering with nuclei in target: **billiard ball collision**
- High mass, low event rate experiments

CDMS

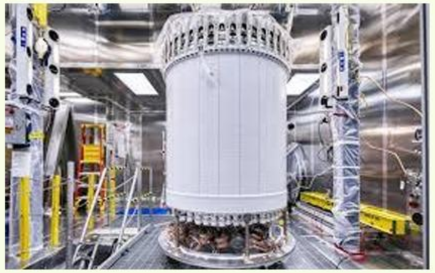

LZ

- Look for annihilation products of dark matter collisions
- Space and land based telescopes
- Typically look in "boosted" signal area (sun or gravitational well where DM collects)

thermal freeze-out (early Univ.)
indirect detection (now)

AMS-02

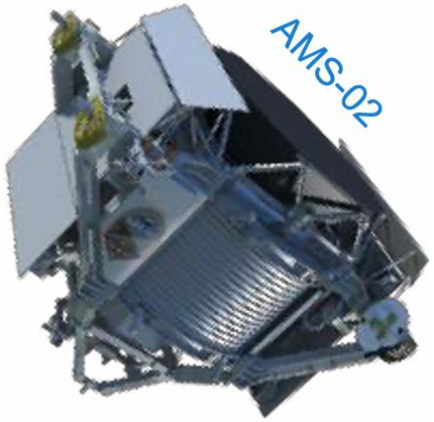

direct detection

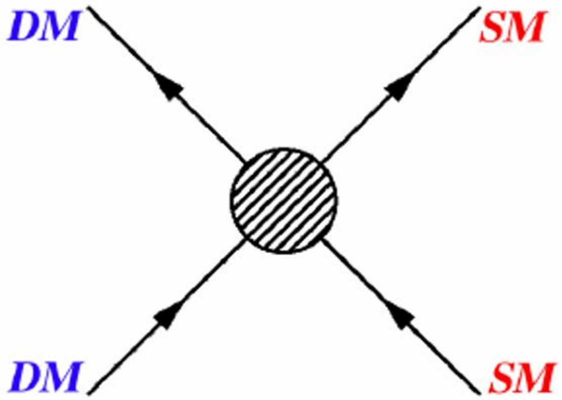

production at colliders

- Produce new particles in high energy collisions

CMS/ATLAS

直接探测暗物质实验

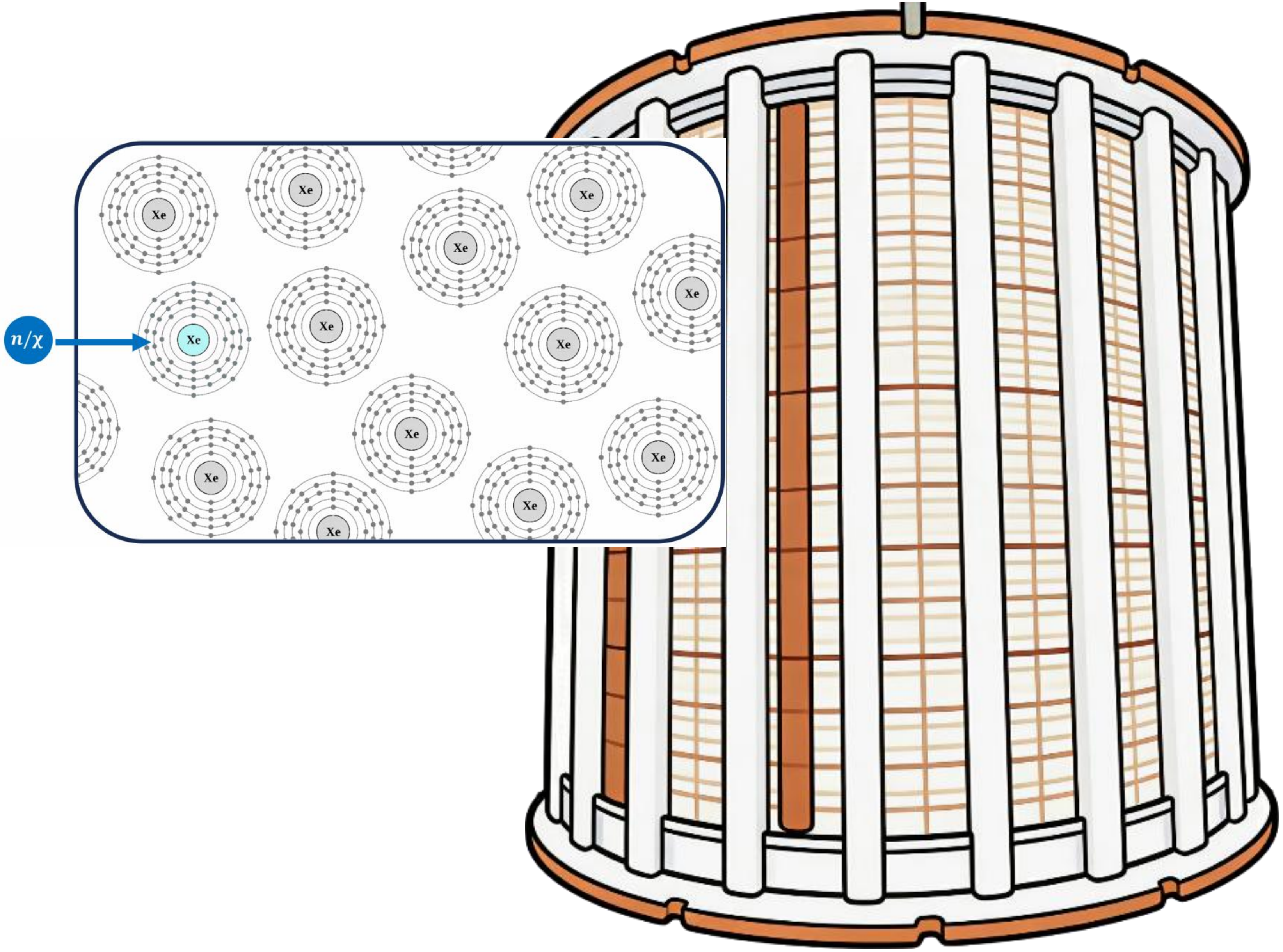

直接探测暗物质实验

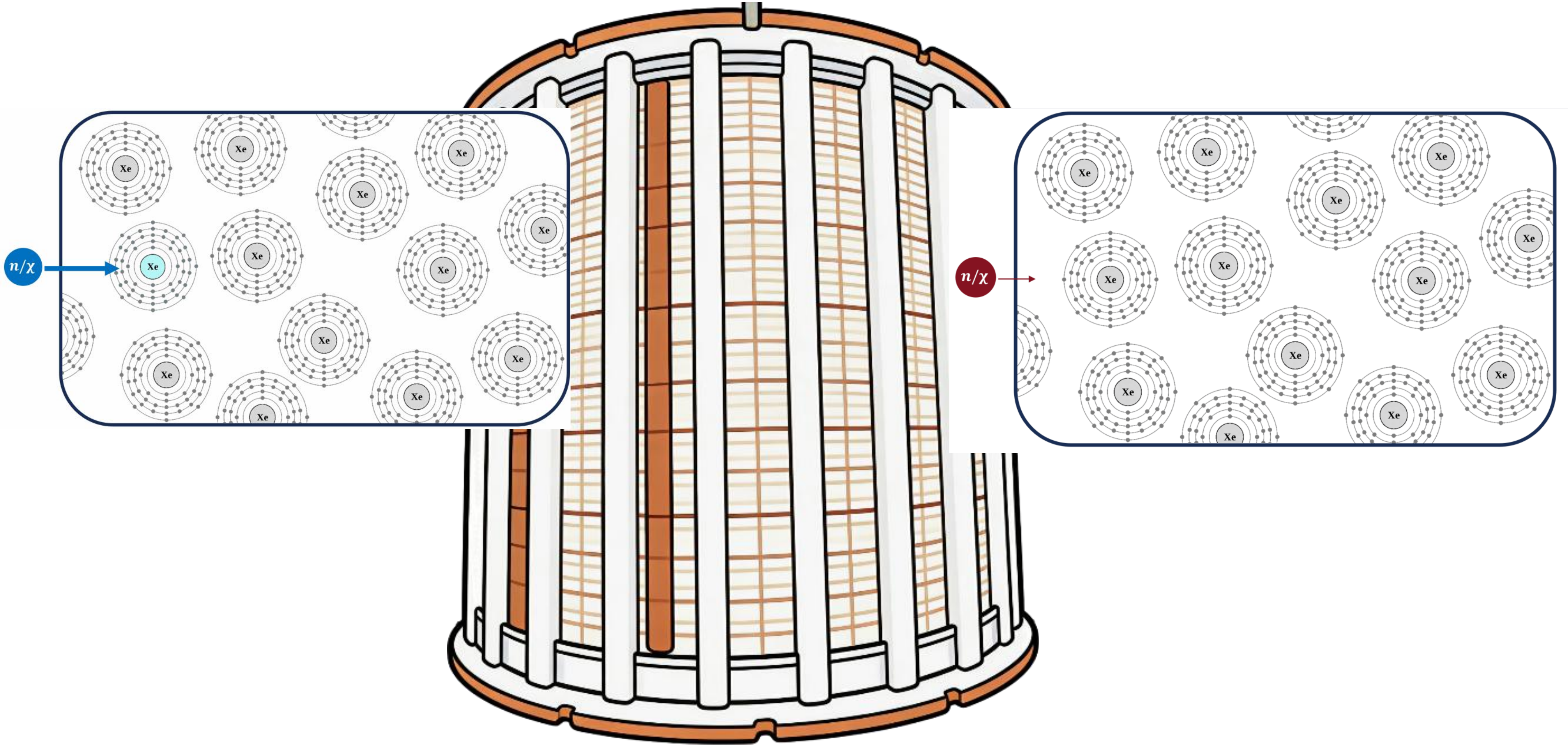

Migdal效应

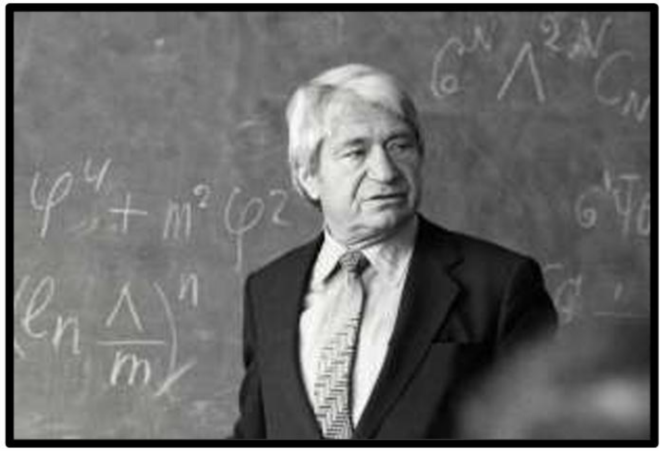

- 1939年由前苏联科学家Migdal预言

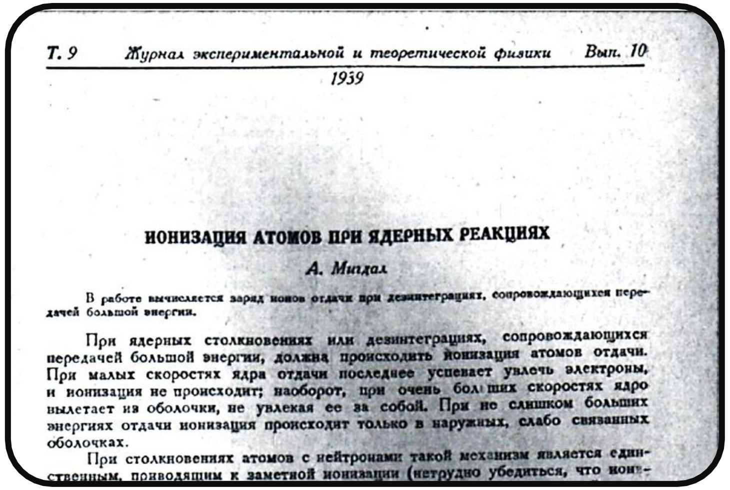

Т. 9 Журнал экспериментальной и теоретической физики Вып. 10

1939

ИОНИЗАЦИЯ АТОМОВ ПРИ ЯДЕРНЫХ РЕАКЦИЯХ

А. Мигдал

В работе вычисляется заряд ионов отдачи при дезинтеграциях, сопровождающихся передачей большой энергии.

При ядерных столкновениях или дезинтеграциях, сопровождающихся передачей большой энергии, должна происходить ионизация атомов отдачи. При малых скоростях ядра отдачи последнее успевает увлечь электроны, и ионизация не происходит; наоборот, при очень больших скоростях ядро вылетает из оболочки, не увлекая ее за собой. При не слишком больших энергиях отдачи ионизация происходит только в наружных, слабо связанных оболочках.

При столкновениях атомов с нейтронами такой механизм является единственным, приводящим к заметной ионизации (нетрудно убедиться, что иони-

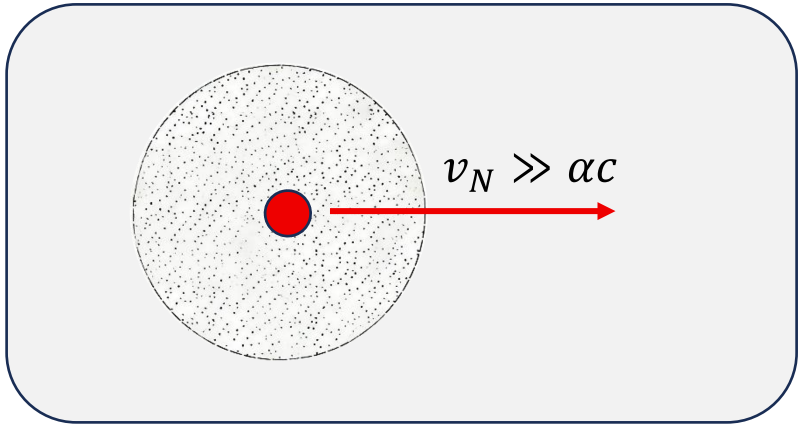

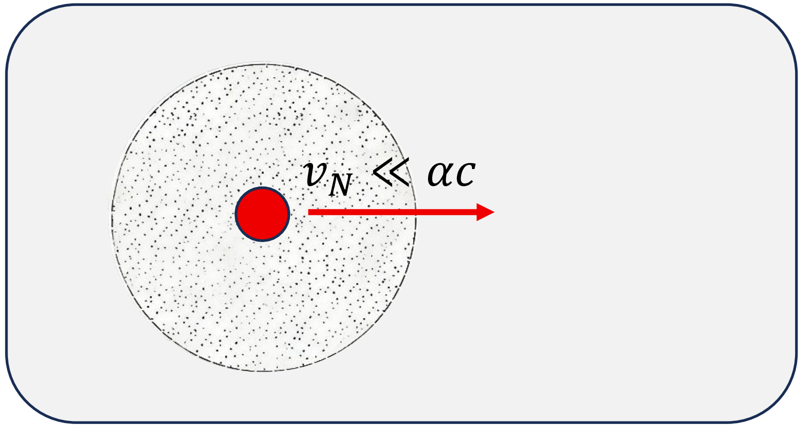

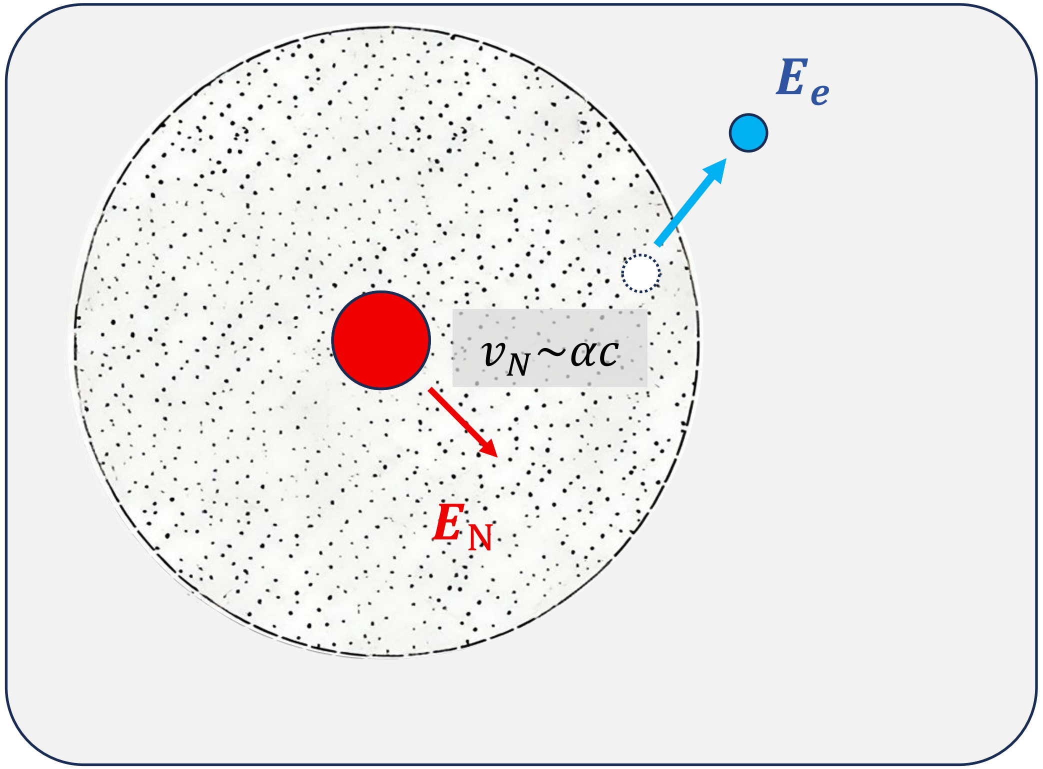

中性粒子碰撞中的Migdal效应

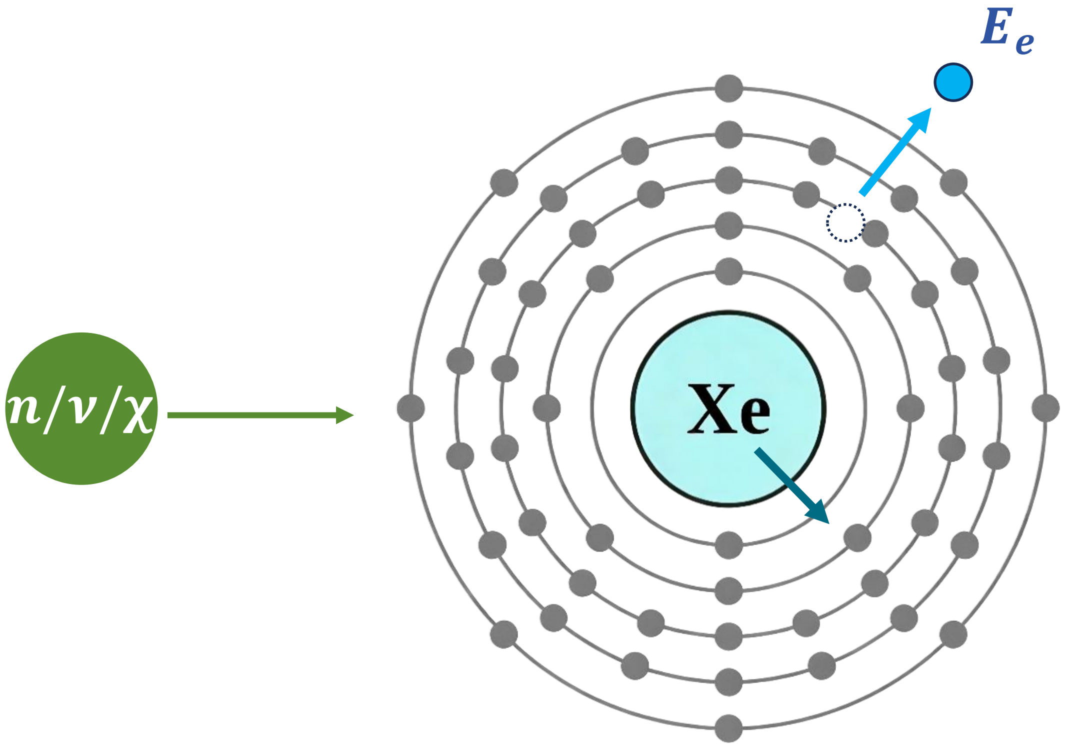

至今已有80余年，仍未有直接观测的证据

利用Migdal效应直接探测暗物质实验

$$E_{er,obs} = E_{er} - E_{bind}$$

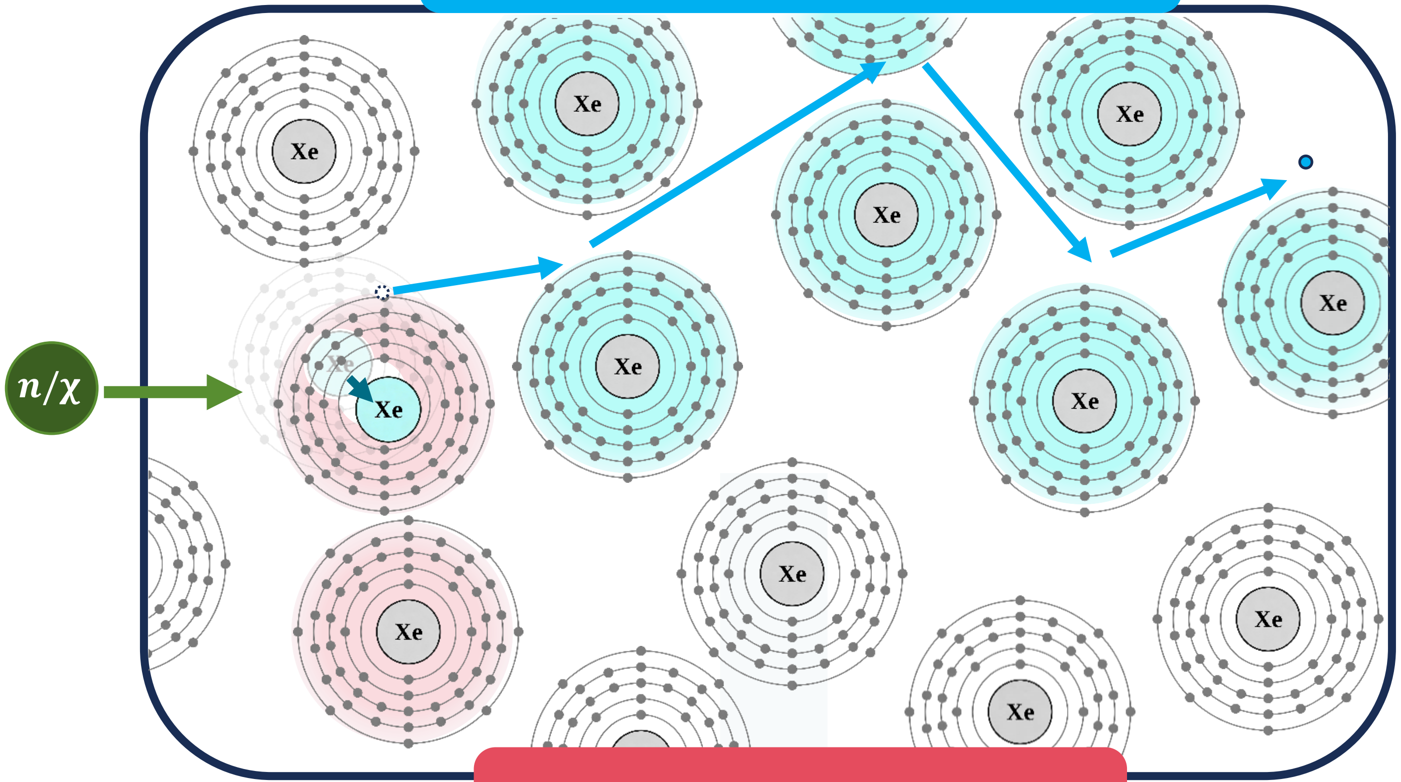

$$E_{nr,obs} = E_{nr} \cdot \varepsilon_{QF}$$

$$E_{det} = E_{er,obs} + E_{nr,obs} + \ldots$$

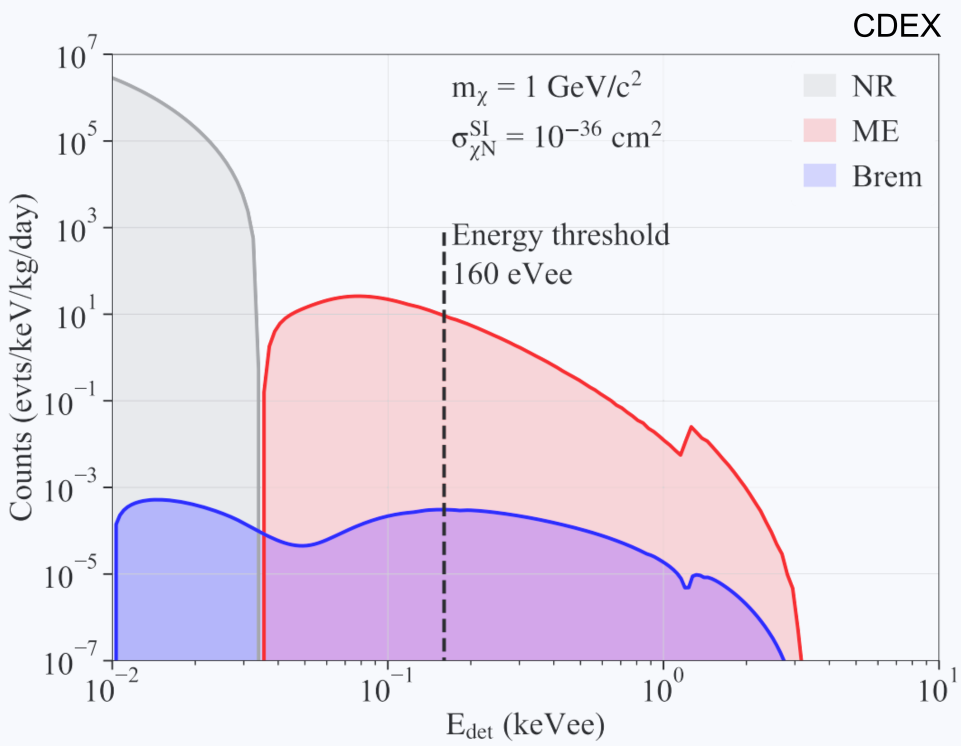

在低动量转移情况下仍然提供可探测信号！

轻质量暗物质区间的探测限—由Migdal效应主导

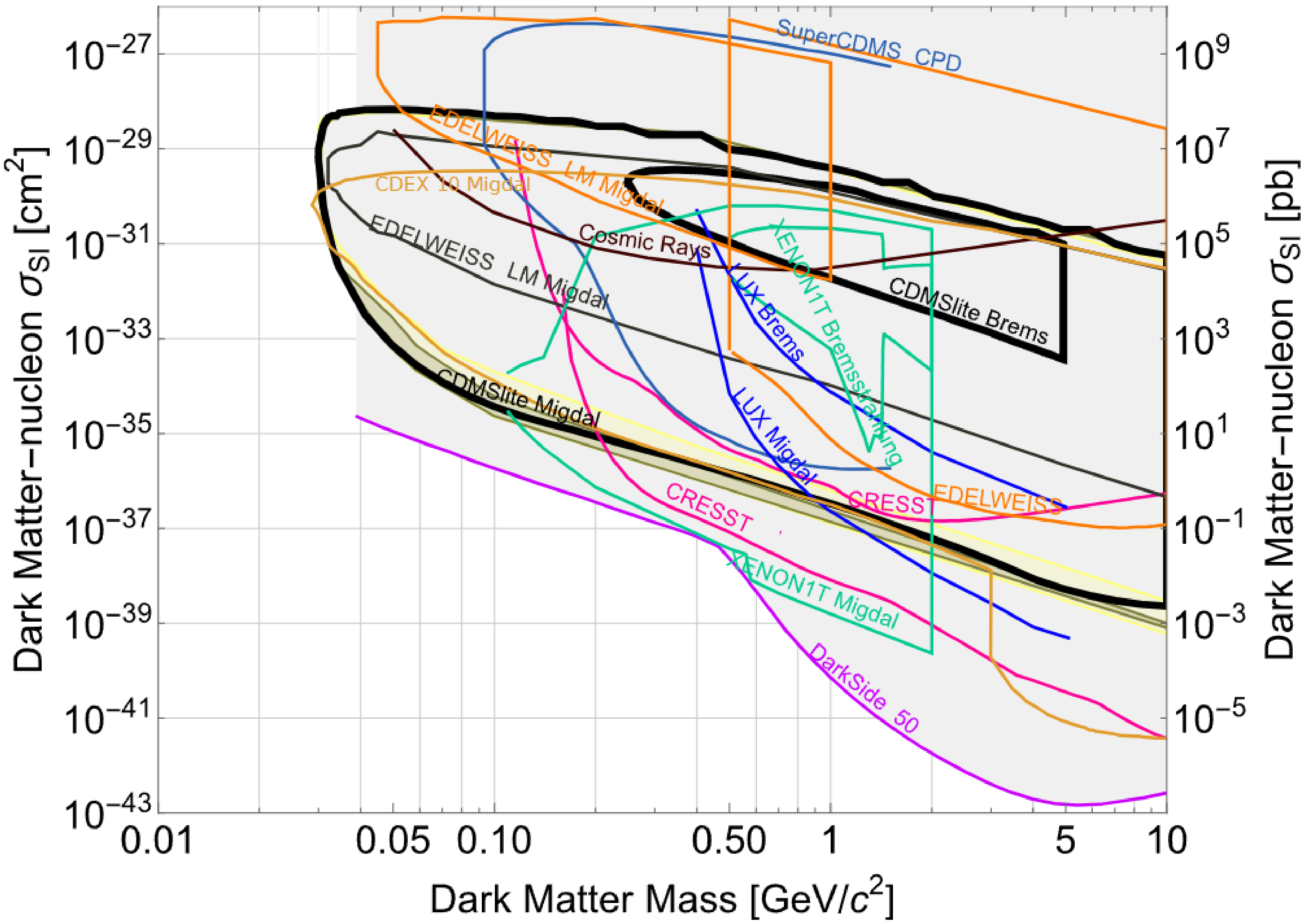

Search for Light Dark Matter Interactions Enhanced by the Migdal Effect or Bremsstrahlung in XENON1T #1
XENON Collaboration • E. Aprile (Columbia U.) et al. (Jul 30, 2019)
Published in: *Phys.Rev.Lett.* 123 (2019) 24, 241803 • e-Print: 1907.12771 [hep-ex]
pdf DOI cite claim reference search 329 citations

Search for new physics in low-energy electron recoils from the first LZ exposure #1
LZ Collaboration • J. Aalbers (SLAC and Stanford U., Phys. Dept. and KIPAC, Menlo Park) et al. (Jul 28, 2023)
Published in: *Phys.Rev.D* 108 (2023) 7, 072006 • e-Print: 2307.15753 [hep-ex]
pdf links DOI cite datasets claim reference search 73 citations

Search for Dark-Matter–Nucleon Interactions with a Dark Mediator in PandaX-4T #1
PandaX Collaboration • Di Huang (Shanghai Jiao Tong U.) et al. (Aug 3, 2023)
Published in: *Phys.Rev.Lett.* 131 (2023) 19, 191002 • e-Print: 2308.01540 [hep-ex]
pdf DOI cite claim reference search 51 citations

Results of a Search for Sub-GeV Dark Matter Using 2013 LUX Data #1
LUX Collaboration • D.S. Akerib (Case Western Reserve U. and SLAC and KIPAC, Menlo Park) et al. (Nov 27, 2018)
Published in: *Phys.Rev.Lett.* 122 (2019) 13, 131301 • e-Print: 1811.11241 [astro-ph.CO]
pdf DOI cite claim reference search 213 citations

Search for Dark-Matter–Nucleon Interactions via Migdal Effect with DarkSide-50 #1
DarkSide Collaboration • P. Agnes (Royal Holloway, U. of London) et al. (Jul 25, 2022)
Published in: *Phys.Rev.Lett.* 130 (2023) 10, 10 • e-Print: 2207.11967 [hep-ex]
pdf links DOI cite claim reference search 107 citations

Search for low-mass dark matter via bremsstrahlung radiation and the Migdal effect in SuperCDMS #1
SuperCDMS Collaboration • M.F. Albakry (British Columbia U. and TRIUMF) et al. (Feb 17, 2023)
Published in: *Phys.Rev.D* 107 (2023) 11, 2023 • e-Print: 2302.09115 [hep-ex]
pdf links DOI cite claim reference search 43 citations

Search for sub-GeV dark matter via the Migdal effect with an EDELWEISS germanium detector with NbSi transition-edge sensors #2
EDELWEISS Collaboration • E. Armengaud (IRFU, Saclay) et al. (Mar 8, 2022)
Published in: *Phys.Rev.D* 106 (2022) 6, 062004 • e-Print: 2203.03993 [astro-ph.GA]
pdf DOI cite claim reference search 66 citations

各大暗物质实验：
XENON/LZ/PandaX/CDEX/DarkSide50/
SuperCDMS/EDELWEISS/LUX…

国际上中性粒子Migdal效应实验

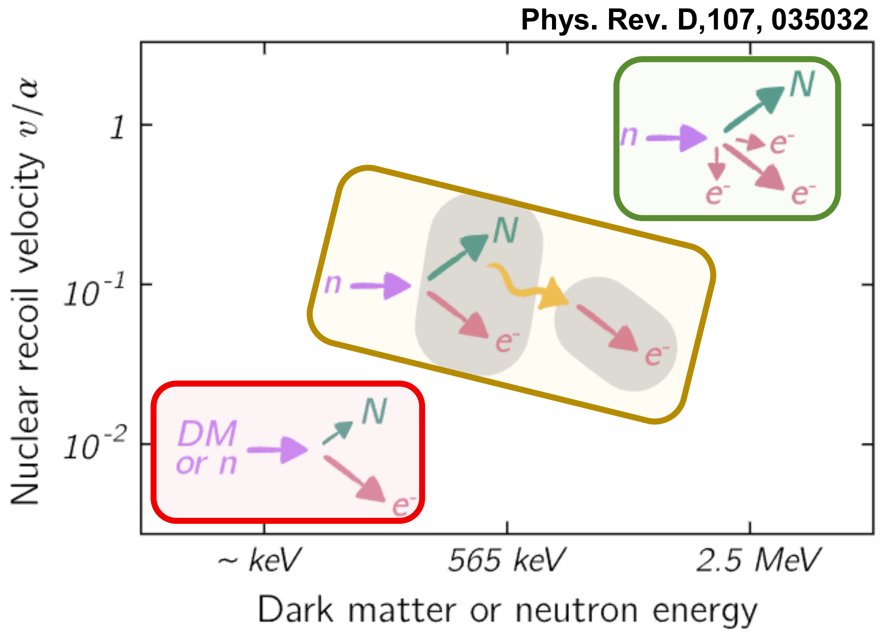

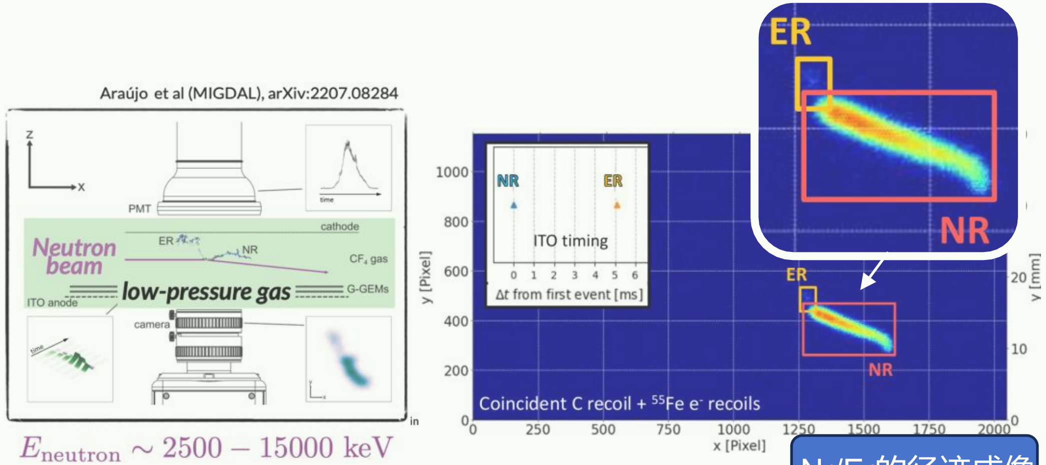

Nr/Er的径迹成像

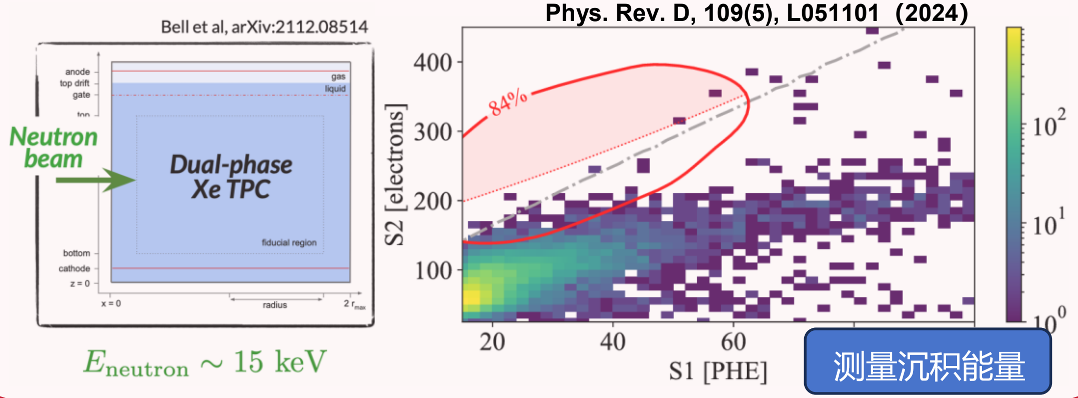

测量沉积能量

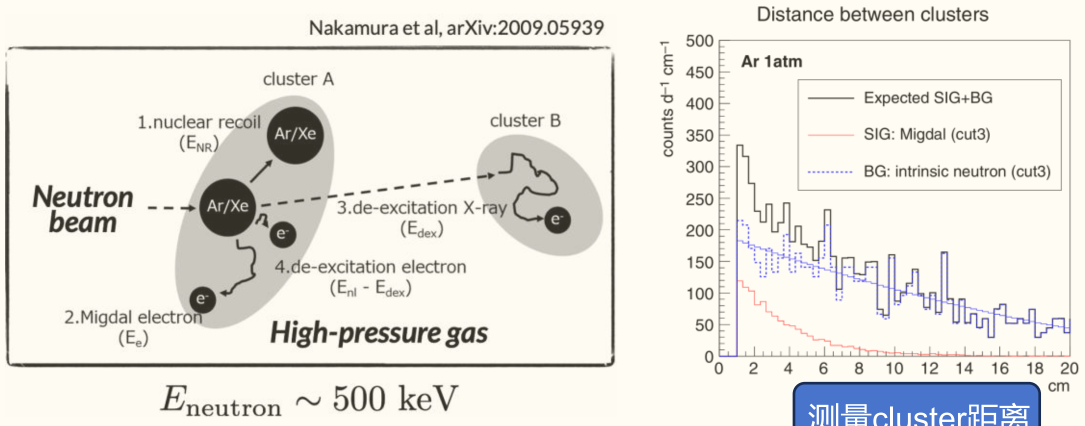

测量cluster距离

Migdal事例的特征

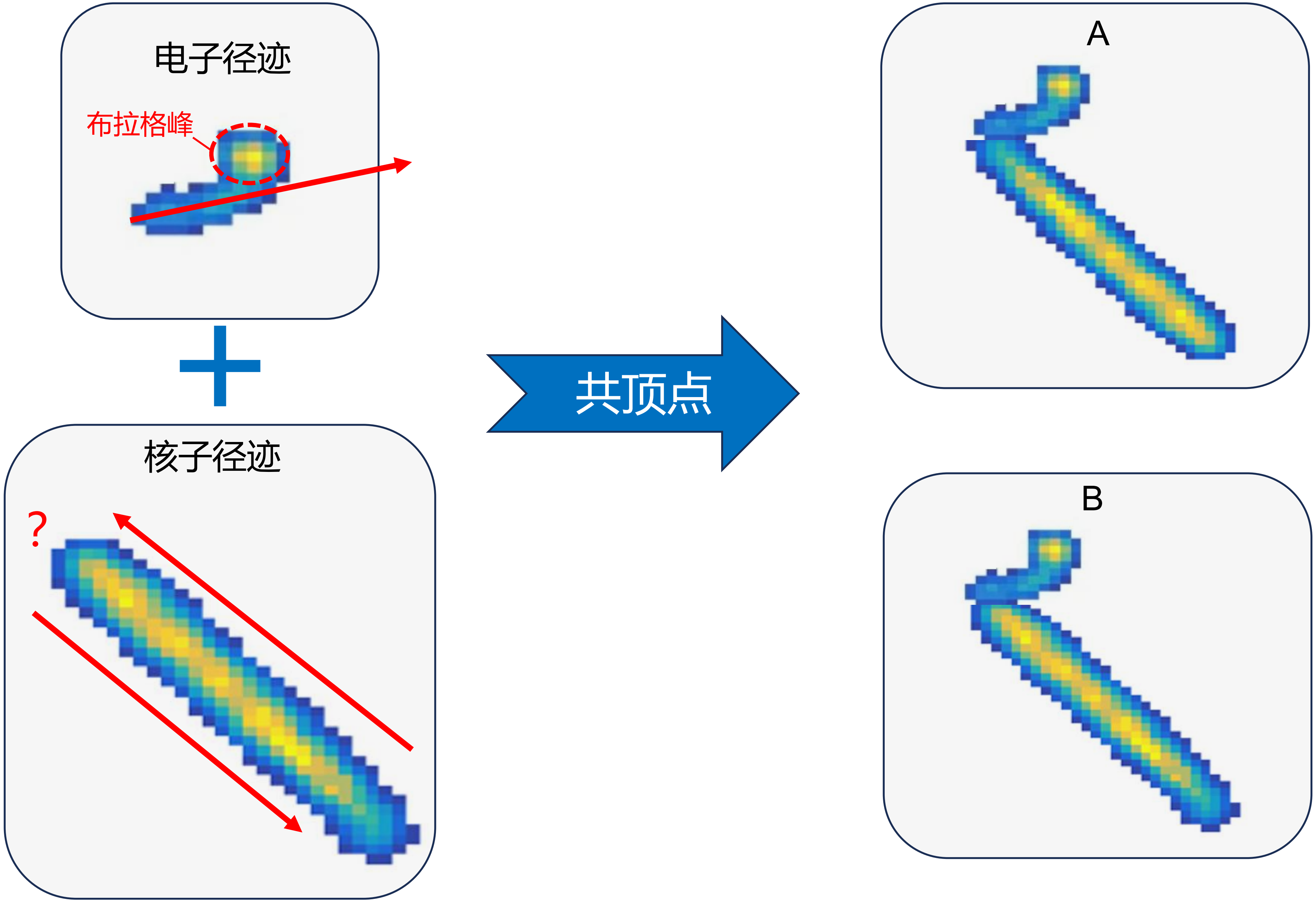

Migdal事例的特征

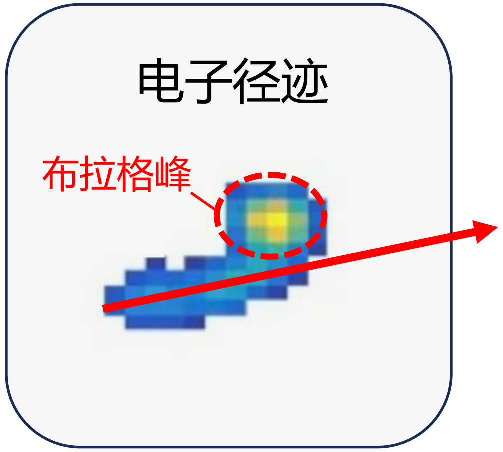

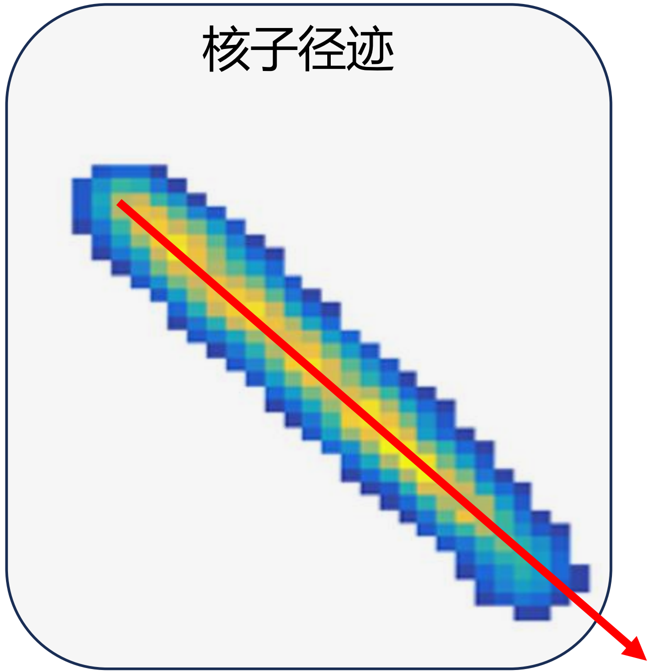

共顶点

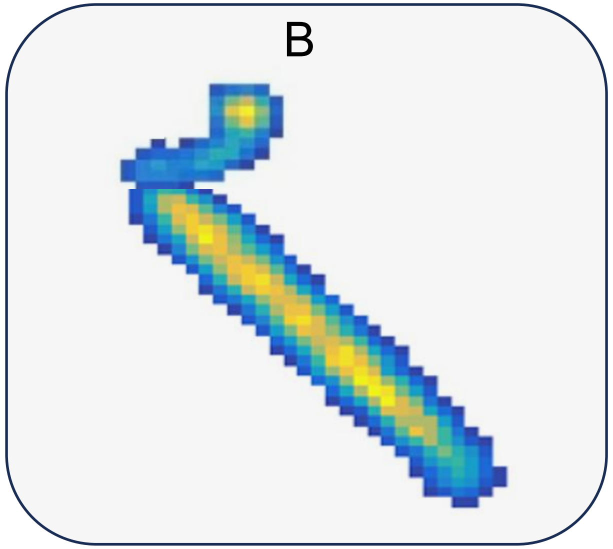

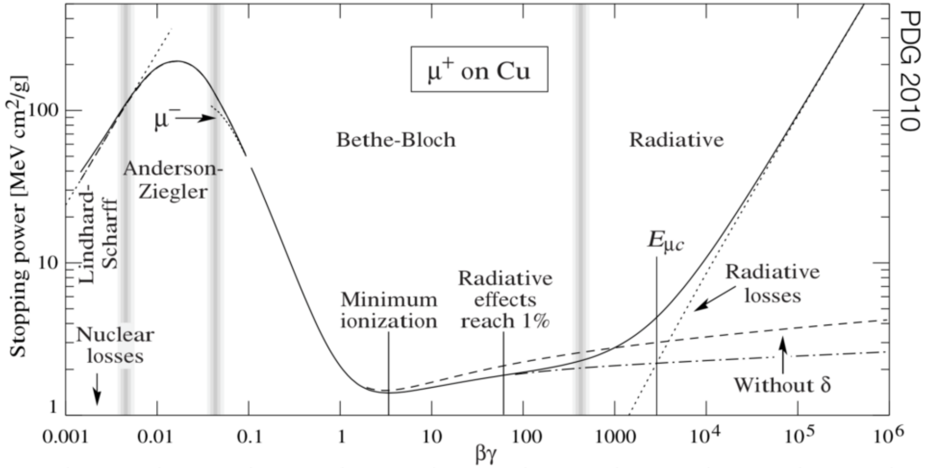

Detector Requirements

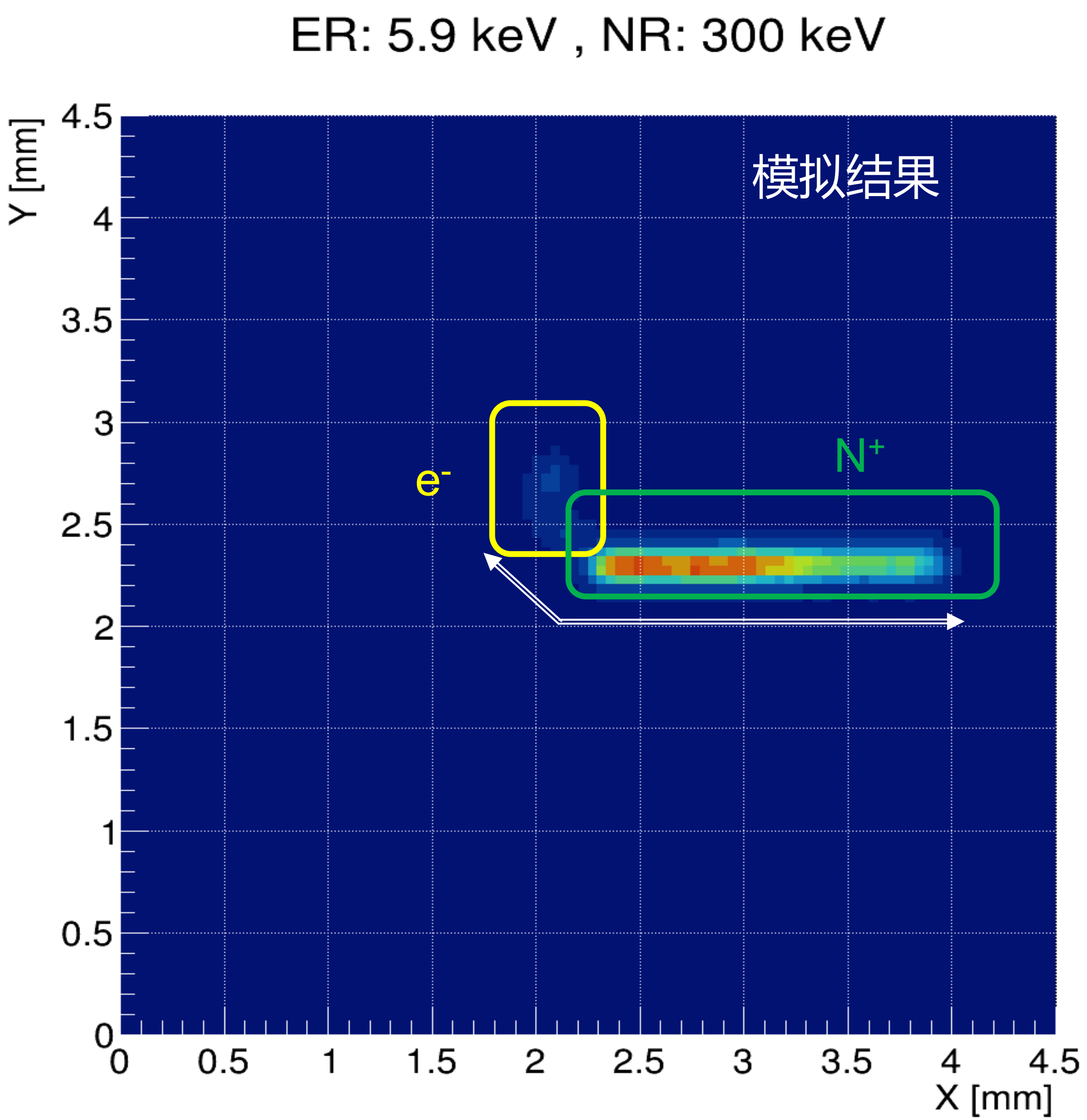

- **ER~keV，NR~hundreds keV**
  - Good energy resolution
  - Large dynamic range.
- **ER shares vertex with NR**
  - Good vertex resolution
- **Reduce possible background**
  - Good time resolution

MARVEL 实验装置示意

GMCP

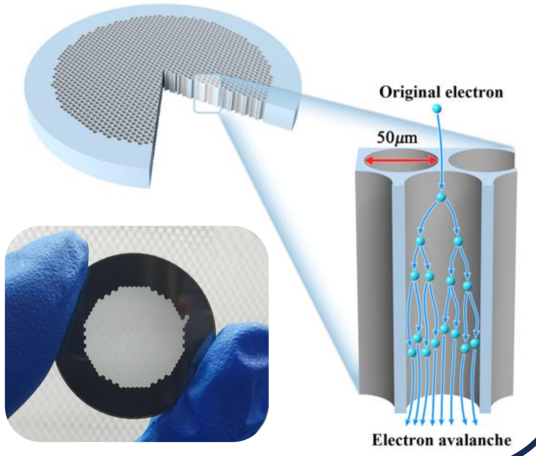

Topmetal-II

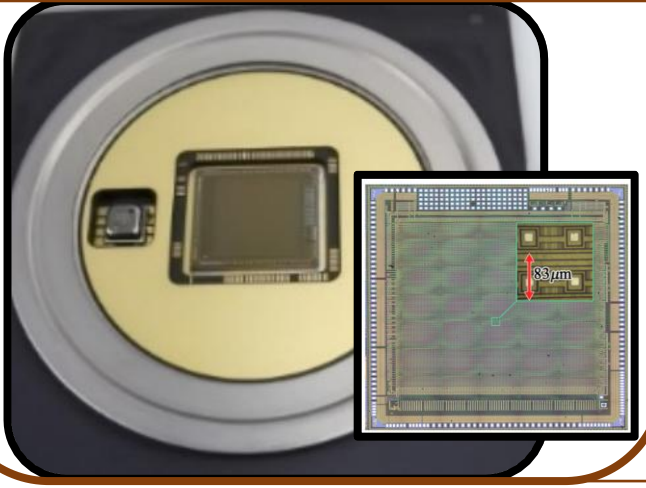

提出全新的实验手段

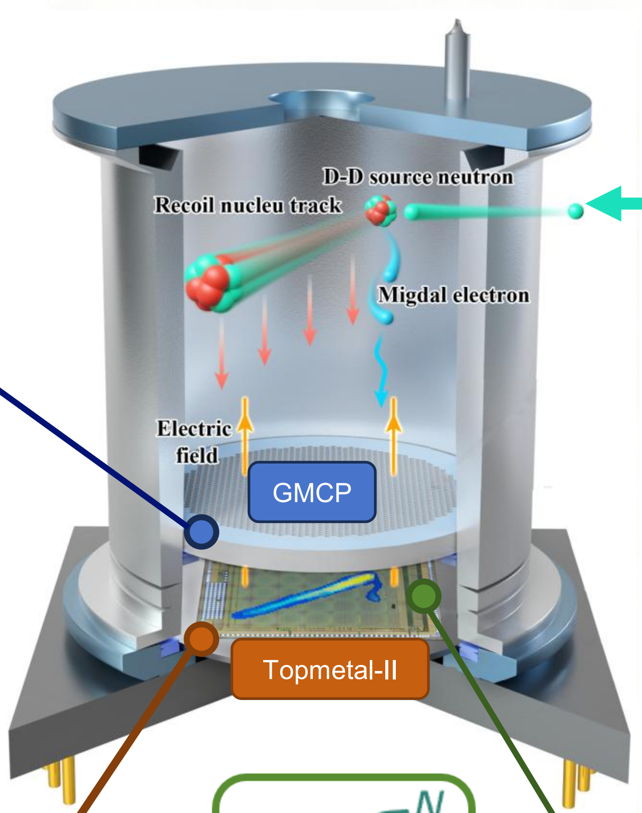

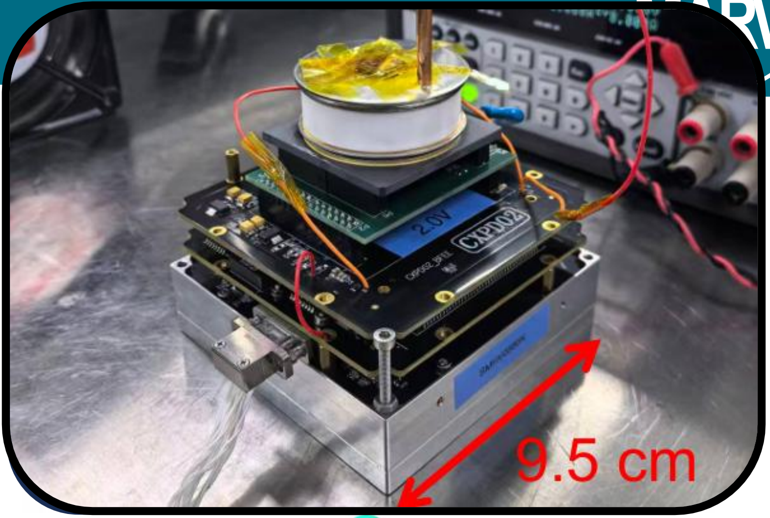

DD neutron source

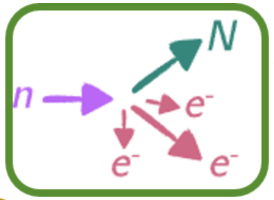

Migdal topology

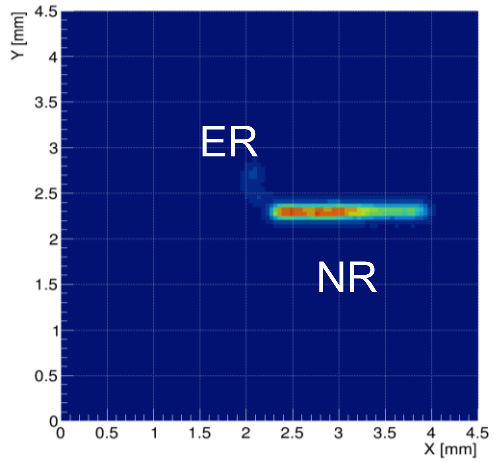

GMCP-Performance Stability

- Suppress the charge accumulation effect

GMCP Development – Hydrogen Reduction tech for Preparing Bulk Resistance to Eliminate Charge Accumulation

Bulk Resistance

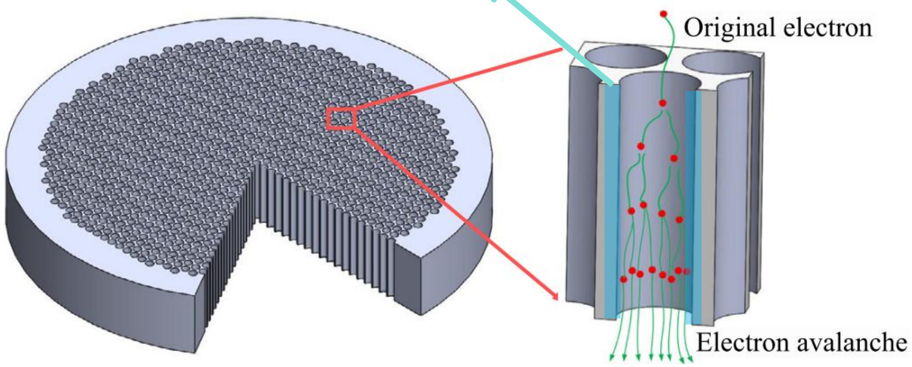

	Type A	Type B	Type C	Type D	Type E
Hole diameter	50 μm	50 μm	50 μm	60 μm	30 μm
Thickness	400 μm	400 μm	300 μm	300 μm	300 μm
Hole pitch	60 μm	60 μm	60 μm	80 μm	40 μm
GMCP resistance	∞	5 GΩ	3 GΩ	5 GΩ	∞
Hydrogen reduction	Without	With	With	With	Without

10.1016/j.nima.2023.168499

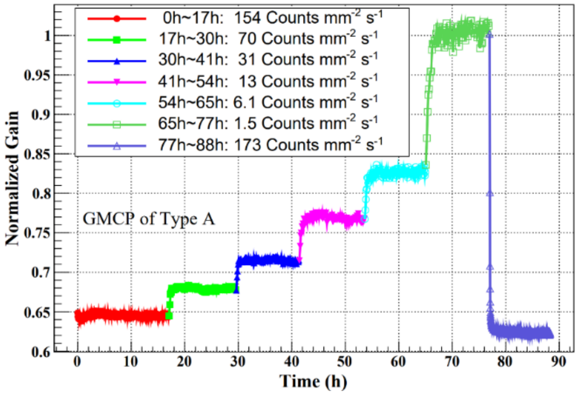

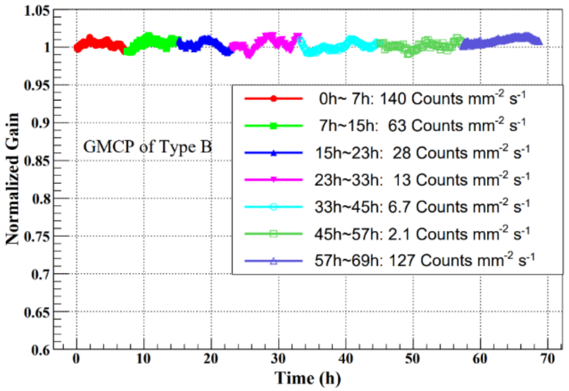

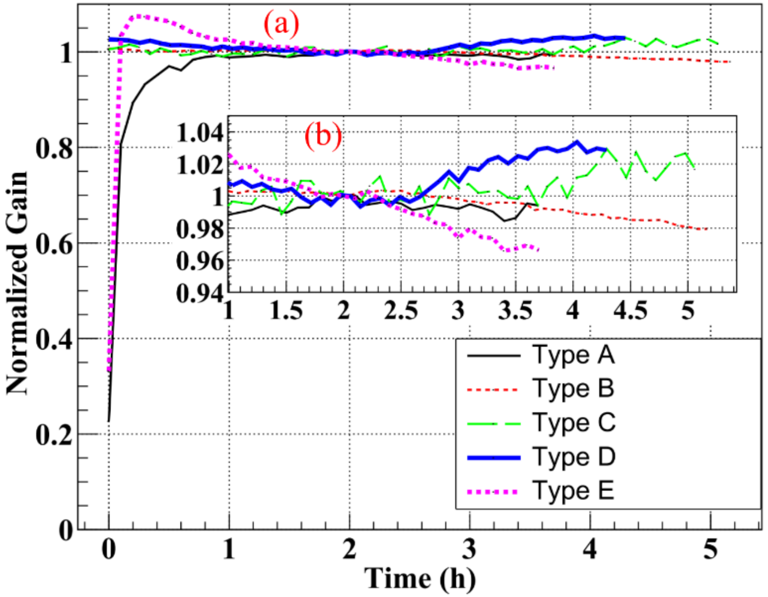

stability at different counting rates

Performance Stability/Gain

- low leakage rate and material degassing rate specifications

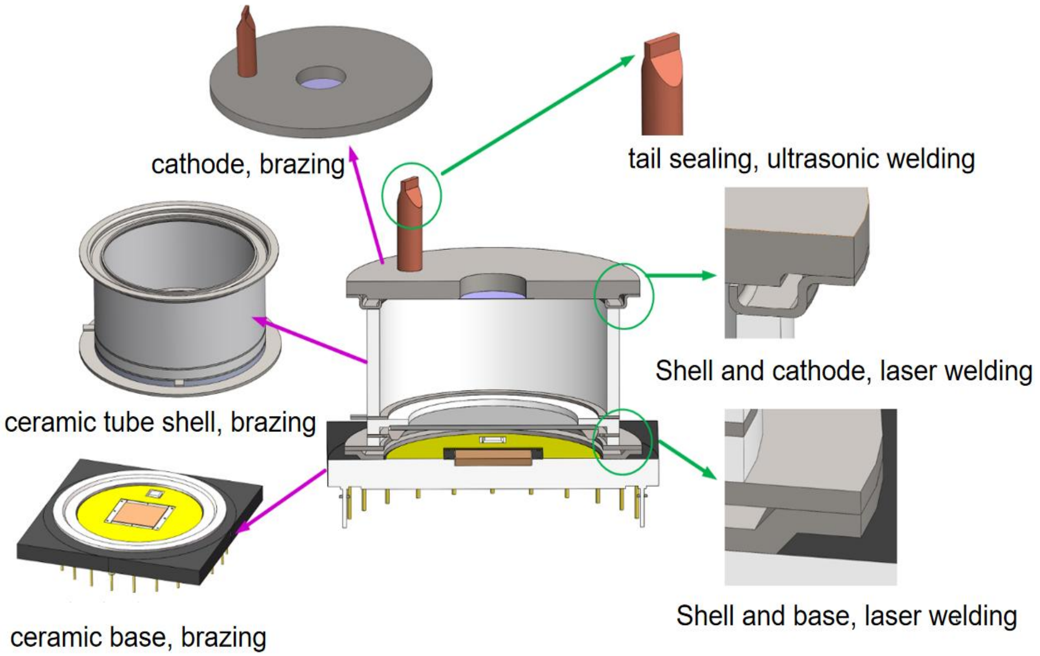

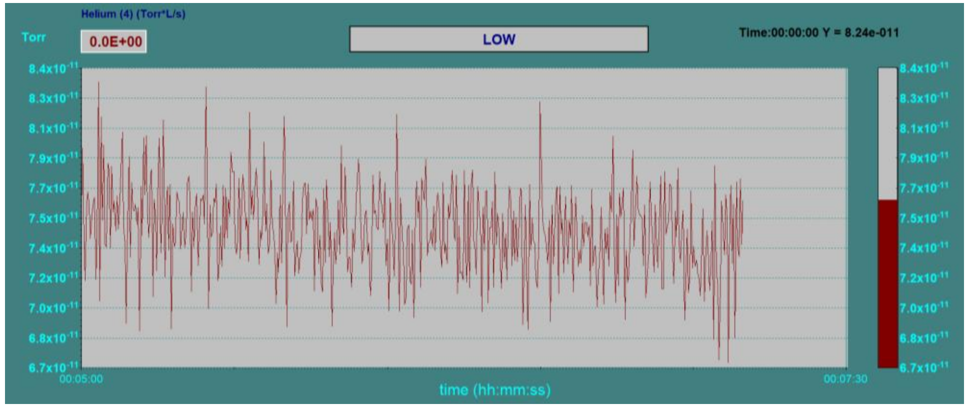

Leak rate: ~7.6^{-11} Torr·L/s

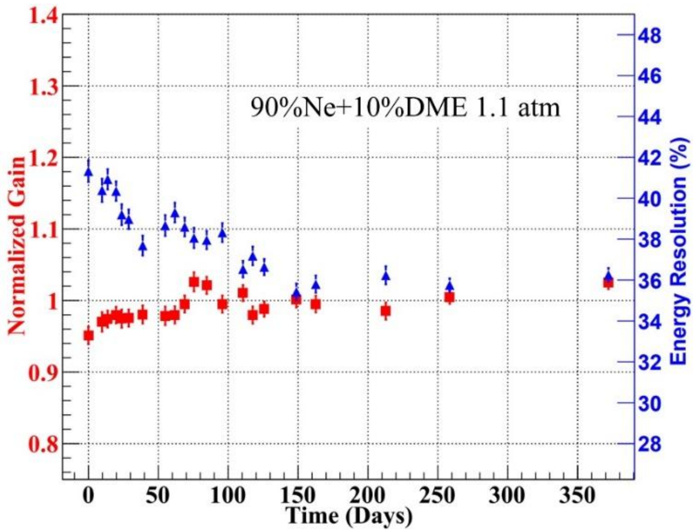

Long-term gain stability

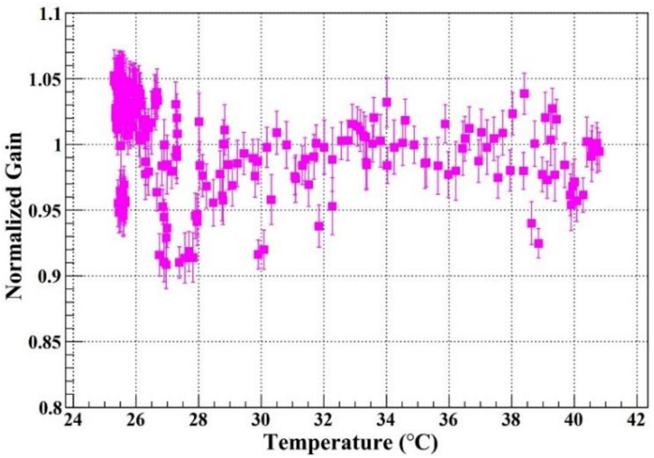

Gain variation with temperature

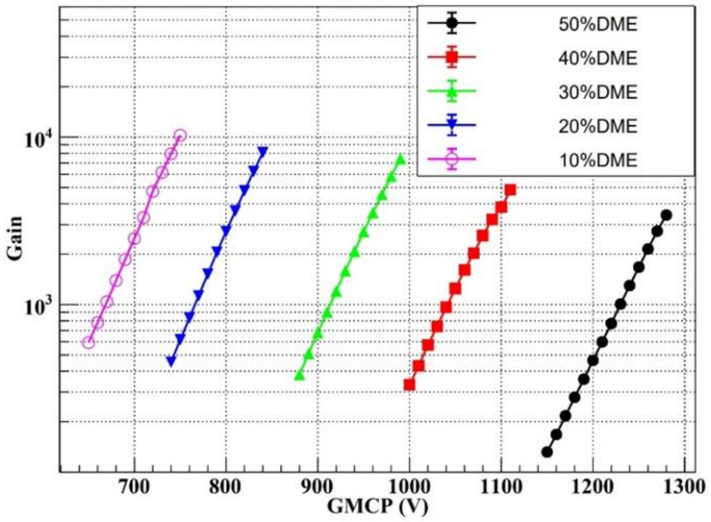

Spatial resolution

various gas mixtures:

He/Ar/Kr/Xe+CO_2/CH_4/i-C_4H_{10}/DME(C_2H_6O)/CF_4

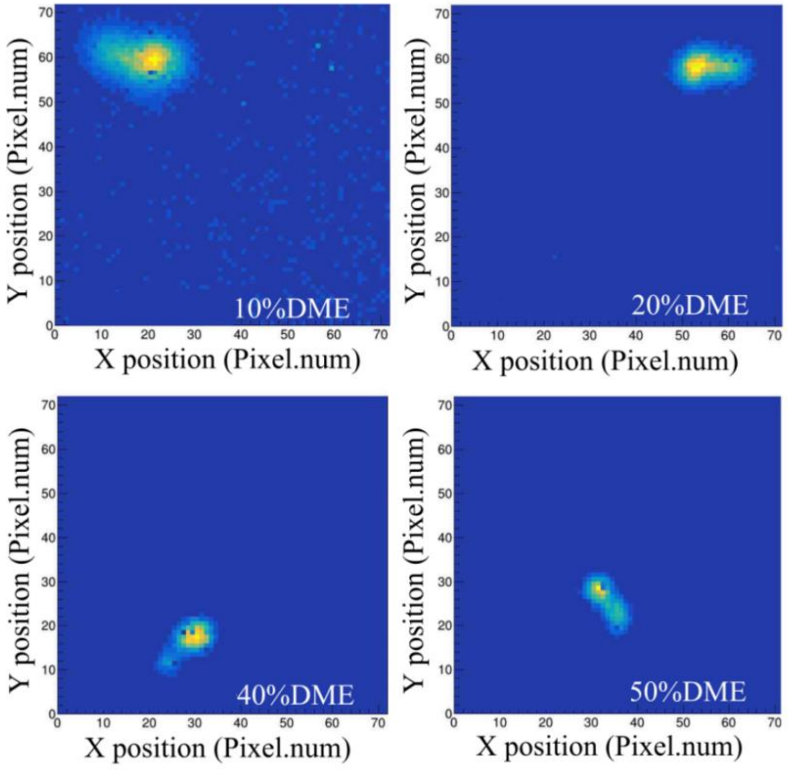

Parameter testing for various gases and gas mixtures

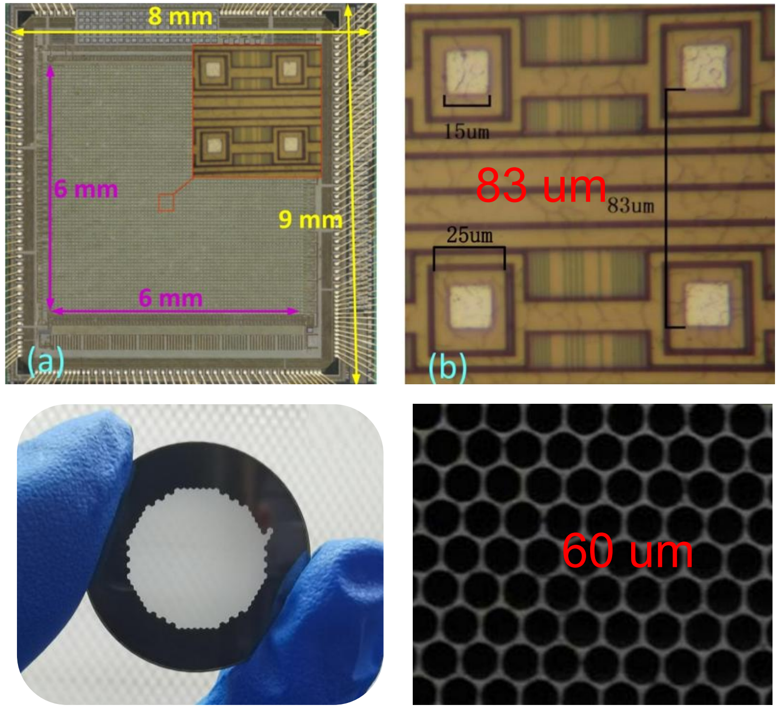

high-granularity device

[10.1007/s41365-021-00903-0](https://doi.org/10.1007/s41365-021-00903-0)

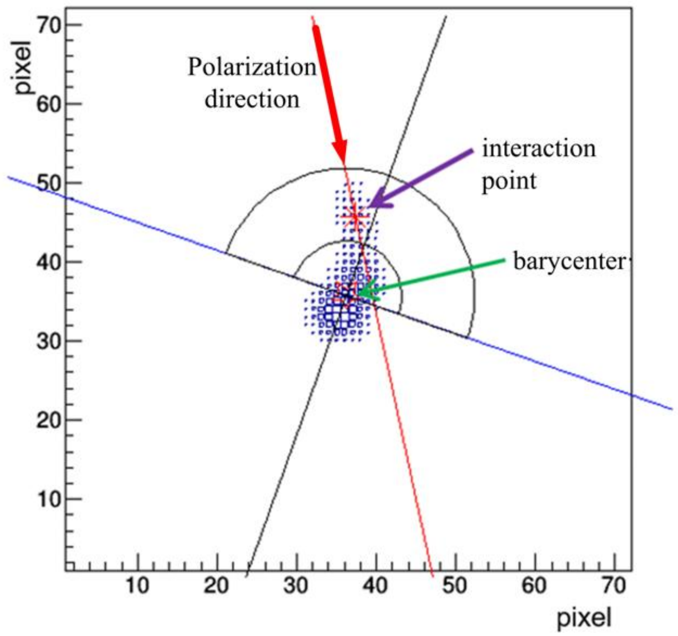

adaptive cutting
vertex reconstruction

ER vertex reconstruction

- Determine the economic center of gravity and its trajectory based on ignition point and energy deposition.

- Calculate the sign of, M_d, $M_d = \sum_{point}(d^3 \times q)$, determine the head and tail(Bragg peak) of the trajectory

- Slide a perpendicular line along the center of gravity, compute the second-order moment M_2 to measure trajectory curvature, and truncate at the point of maximum M_2 change for a straightened path.

$$M_2 = \sum_{n}^{\text{pixels}} (x_n - x_l)^2 + (y_n - y_l)^2$$

- Recalculate the center of gravity and its line for the truncated trajectory to identify the photoelectric interaction point and emission direction.

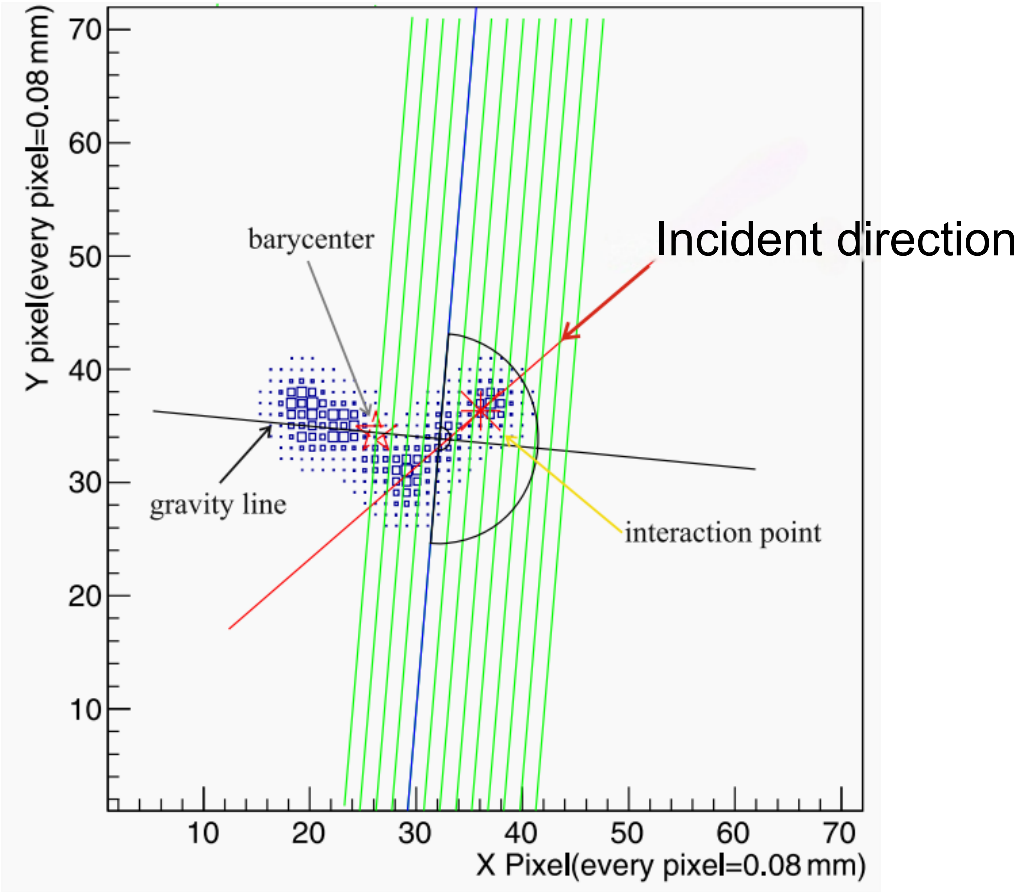

21

Vertex resolution

copper plate

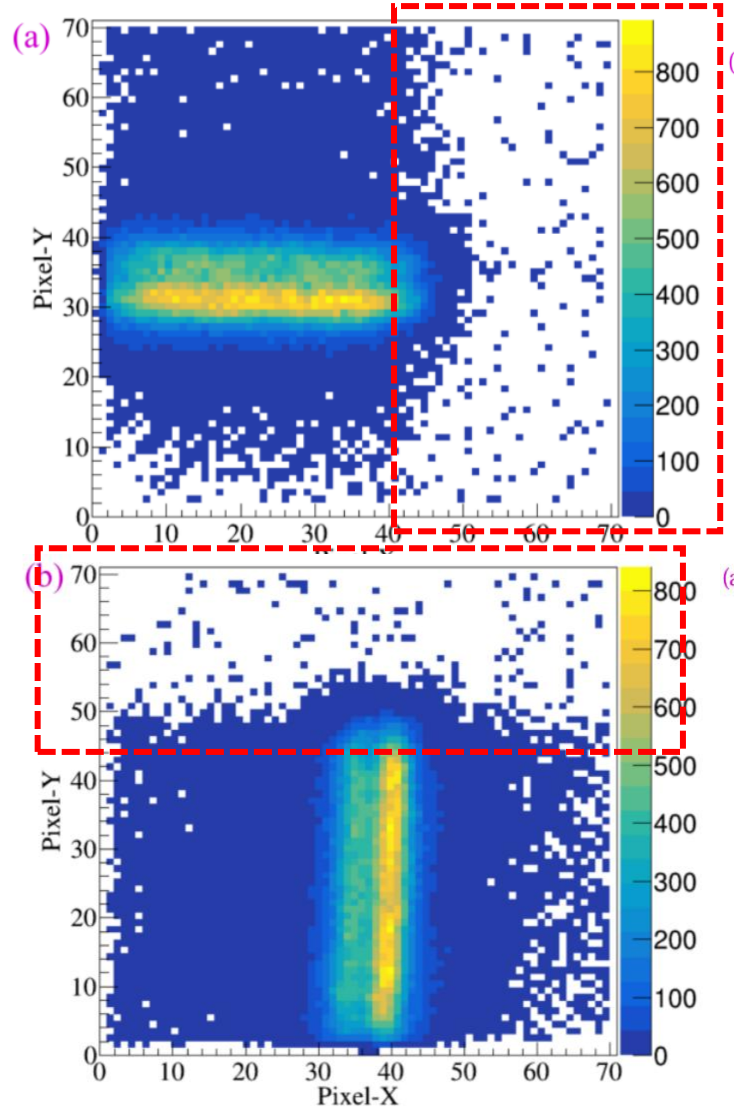

6.4 keV X-ray imaging with half the area shielded by a copper plate

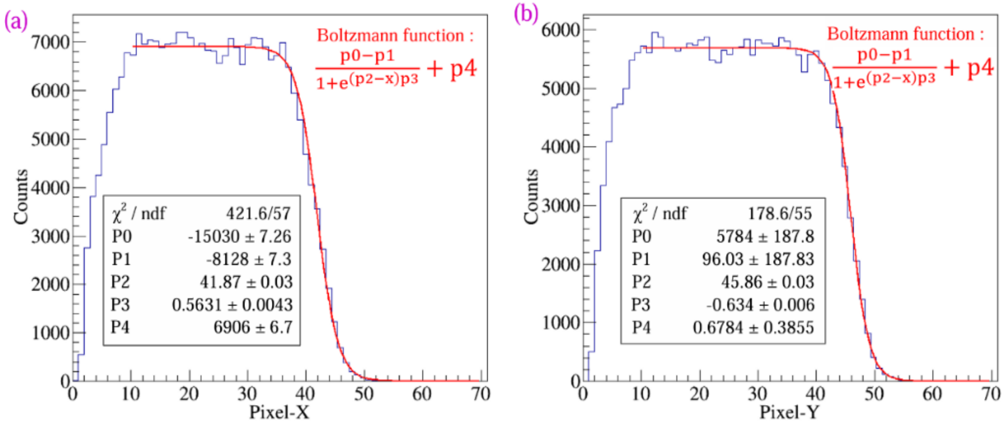

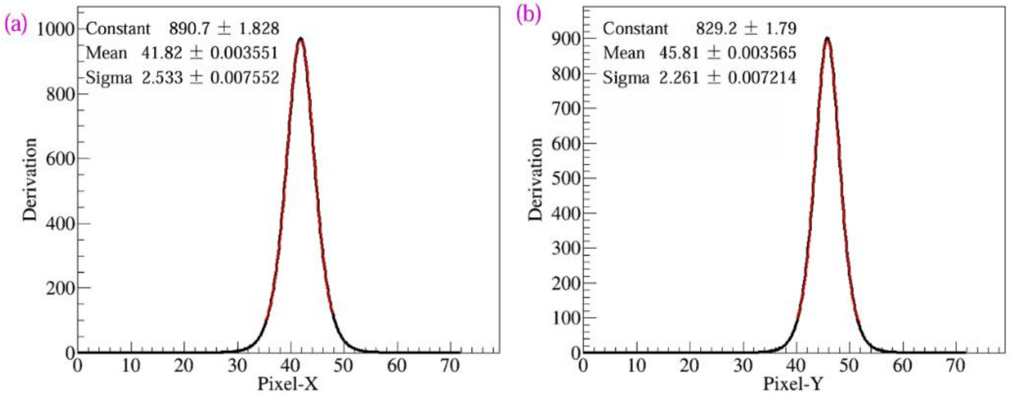

position resolution @ 6.4 keV

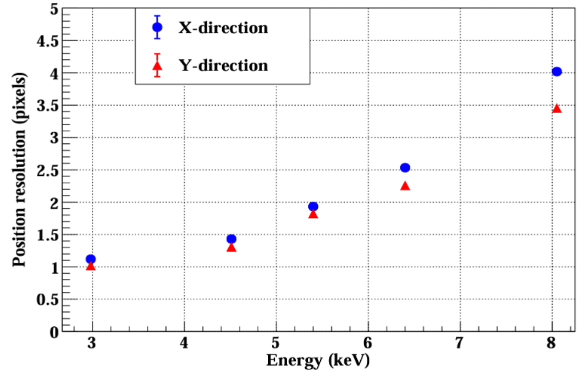

position resolution at different energies

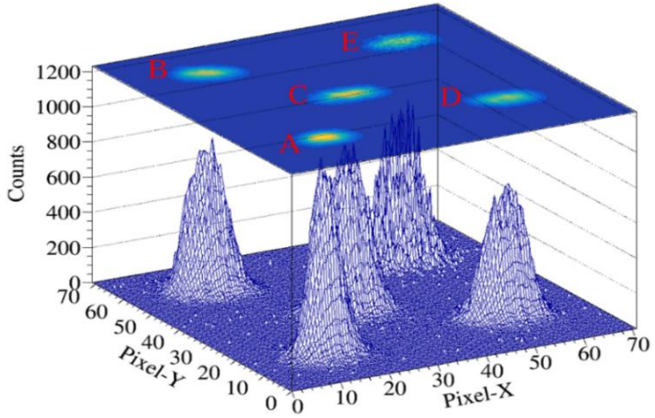

spatial resolution at different positions

10.1088/1748-0221/19/04/P04039

Energy calibration

Energy (keV)	Crystal	Incident radiation	Diffraction angle(deg)
2.98	Si(111)	Ag L_α	41.6
4.51	Si(220)	Ti K_α	45.8
5.40	Si(311)	Cr K_α	44.5
6.40	Si(400)	Fe K_α	45.5
8.05	Si(224)	Cu K_α	44.1

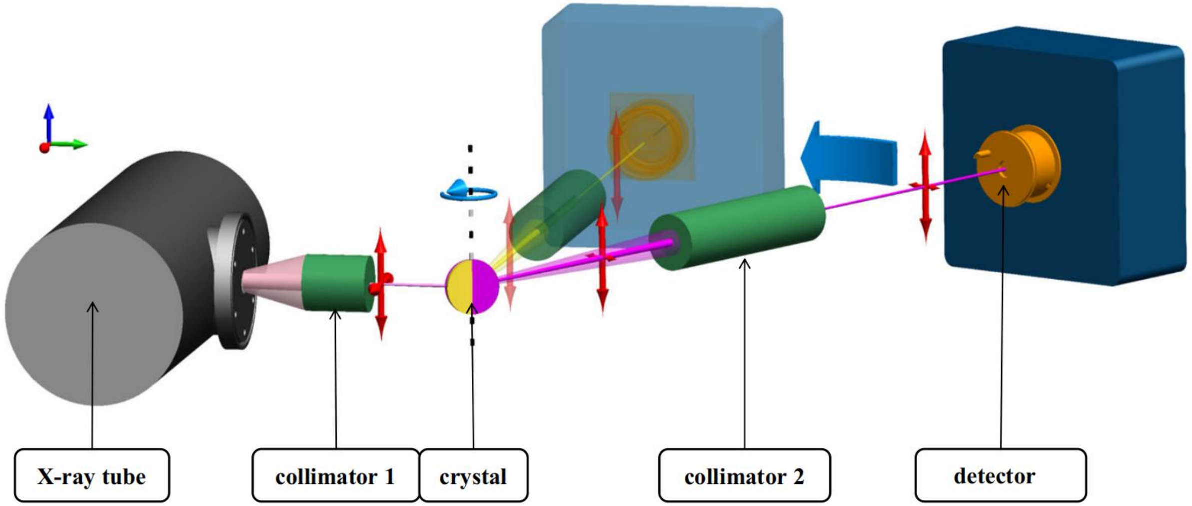

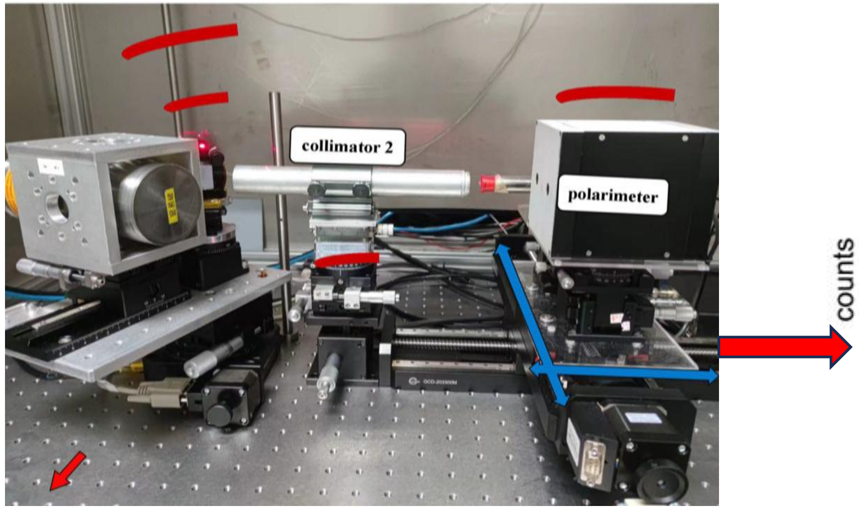

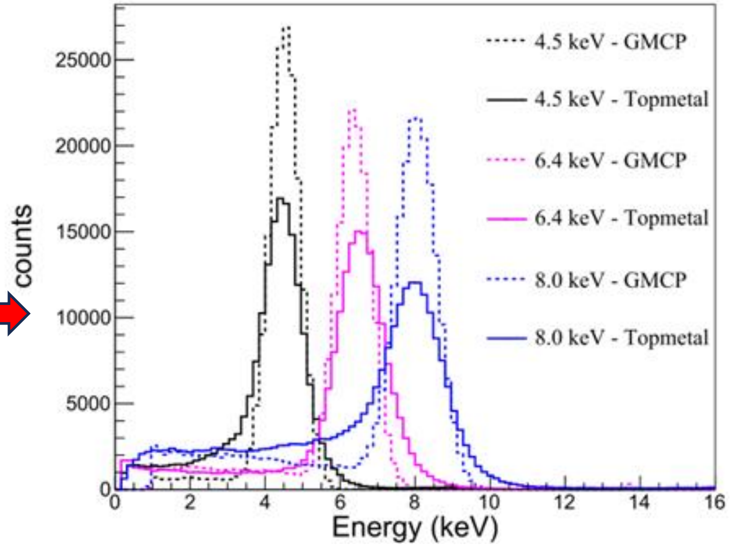

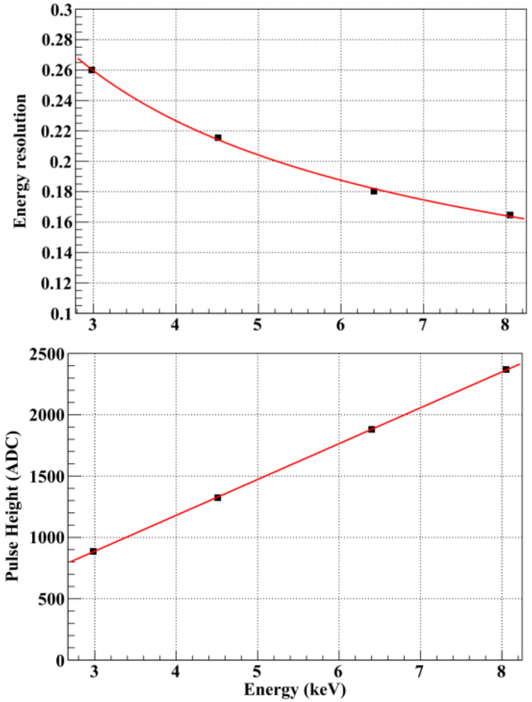

$\propto 1/\sqrt{E}$

10.1007/s10686-023-09905-9

monoenergetic X-ray platform

Time resolution

GMCP trigger : 100 Mhz (10 ns)

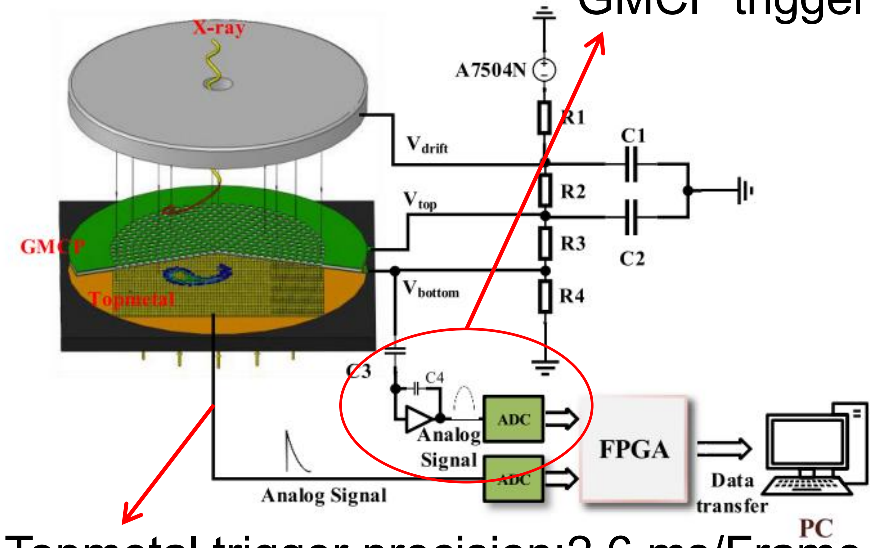

Topmetal trigger precision:2.6 ms/Frame

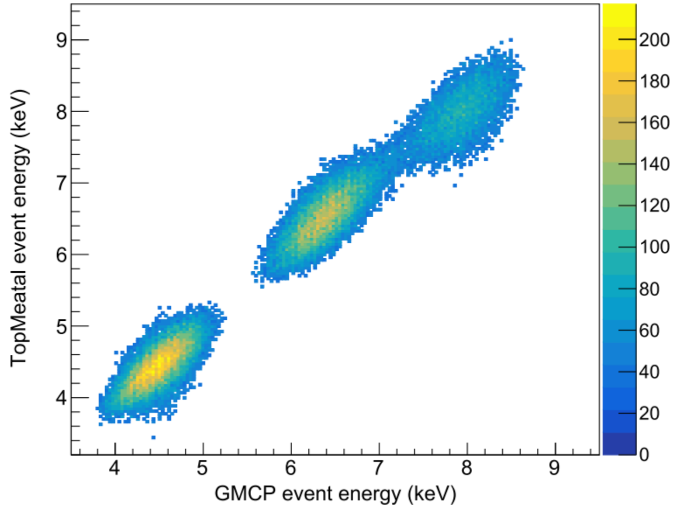

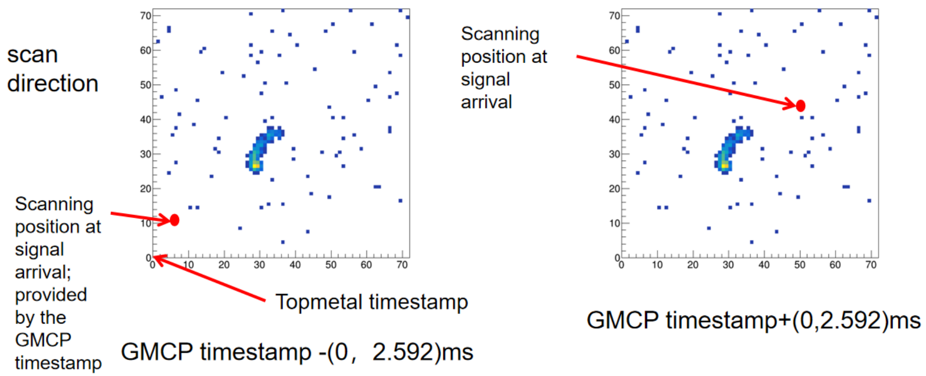

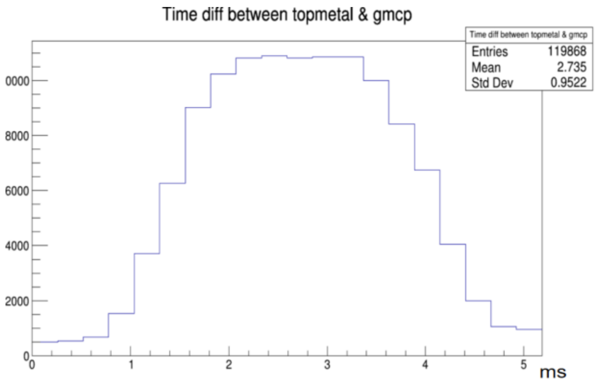

6 ms Timewindow

IEEE Trans. Nucl. Sci., 70, 1288-1295

deltaT = $t_{topmetal}-t_{GMCP}$+Pixel_order*500ns

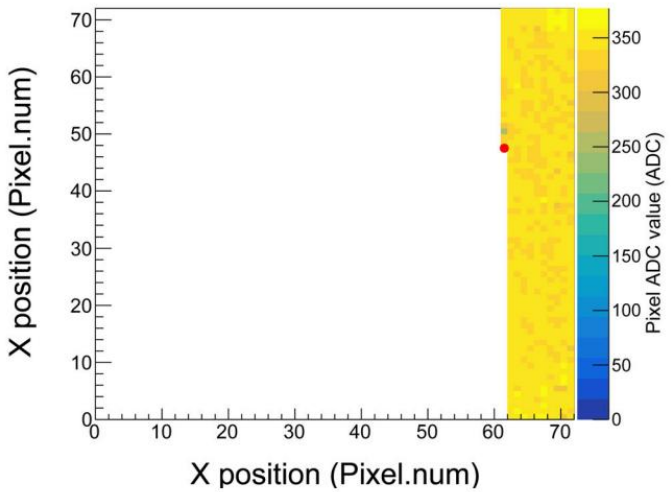

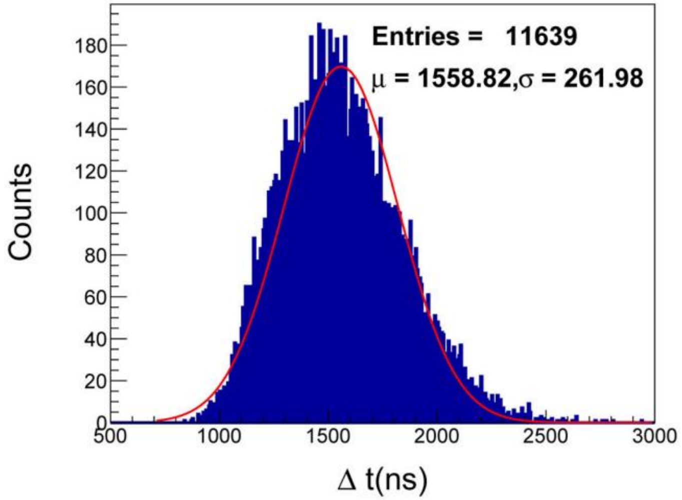

time resolution test results

Events discrimination at same frame

scan direction

Scanning position at signal arrival; provided by the GMCP timestamp

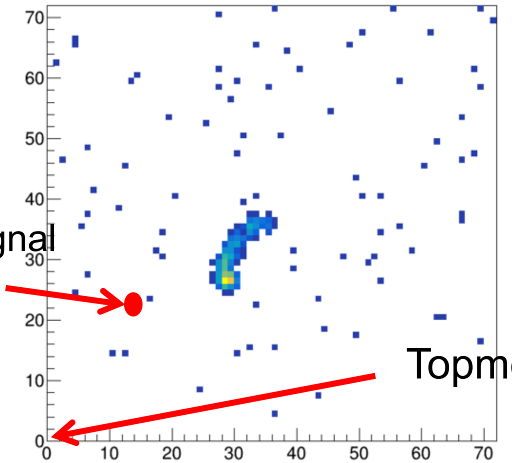

Topmetal timestamp

GMCP timestamp-(0,2.592)ms

Scanning position at signal arrival

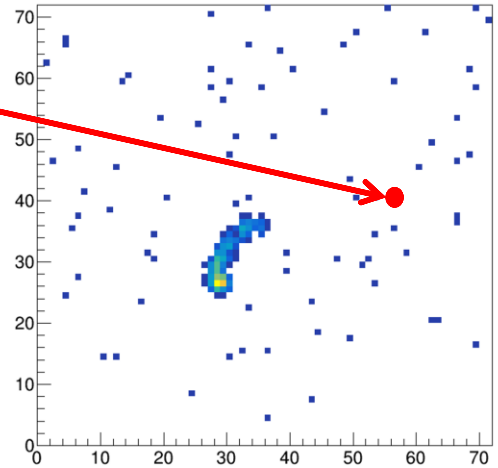

GMCP timestamp+(0,2.592)ms

Frame ***N***

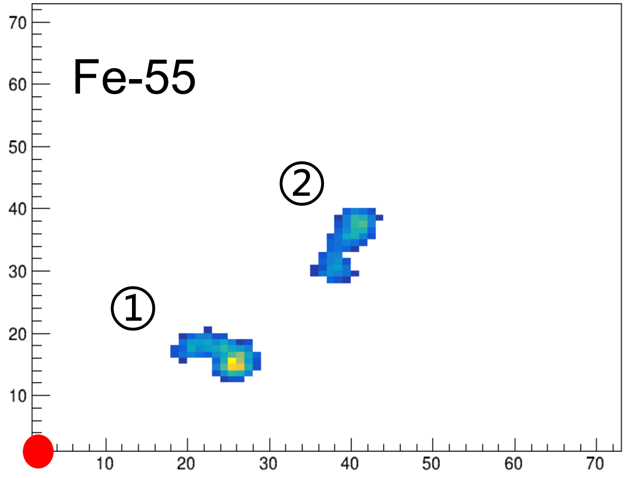

T_N =17.96207 s

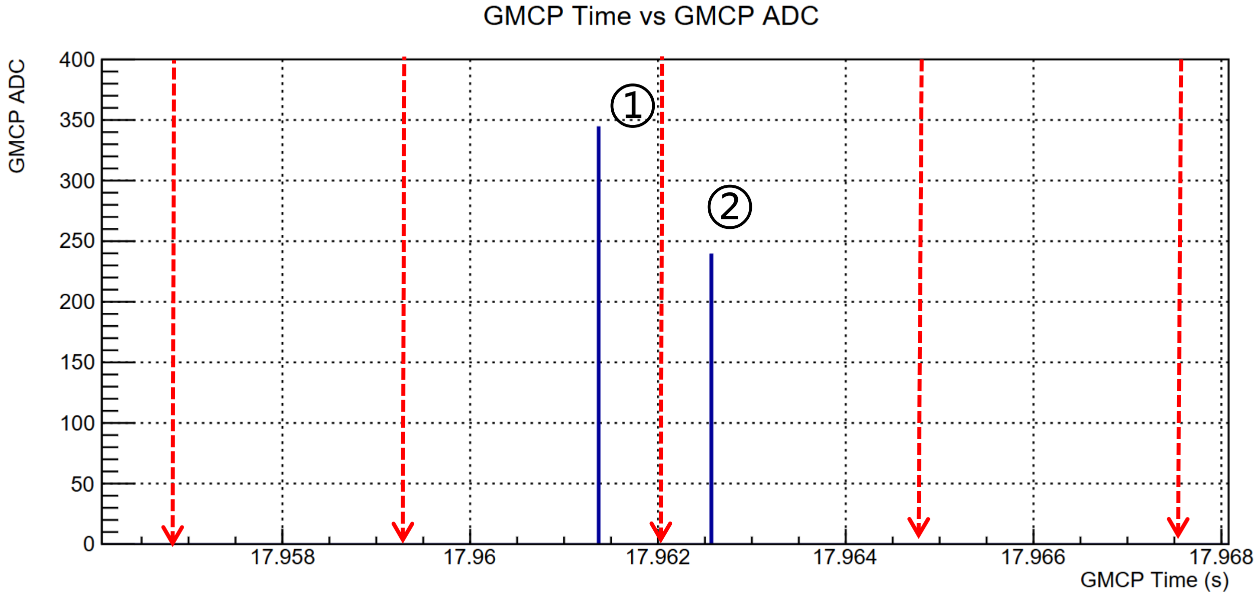

… T_{N-1} T_N T_{N+1} …

Detector performance

Energy resolution

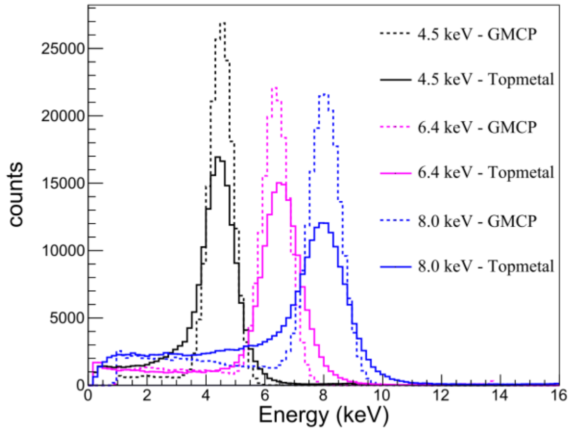

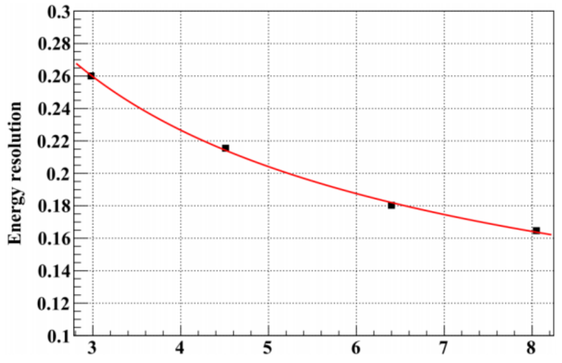

- Good linear energy response
- 20%-30% energy resolution(FWHM)
- Energy resolution follows the relationship ~ $1/\sqrt{E}$

Dynamic range

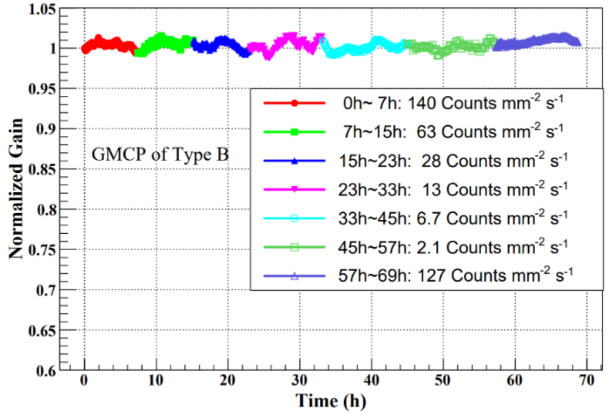

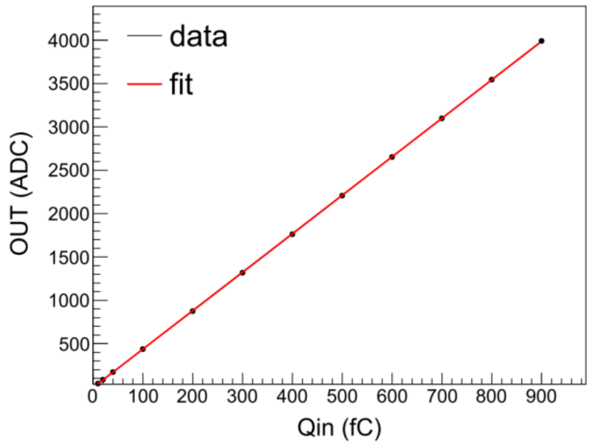

- Stable gain under different count rates(no pile up)
- Good linearity in charge response

Vertex resolution

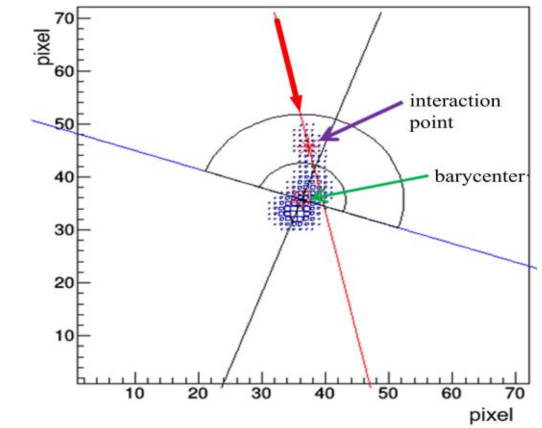

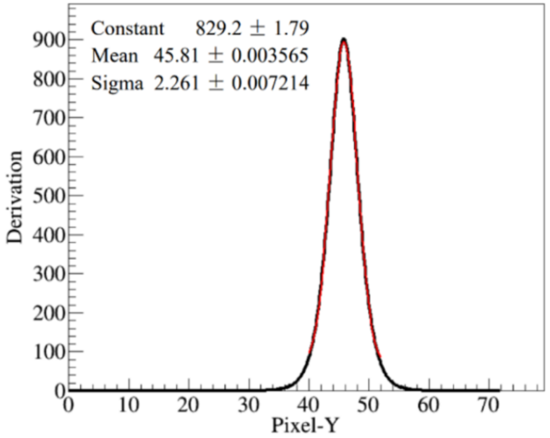

- ~200 μm vertex resolution @ 6.4 keV

Time resolution

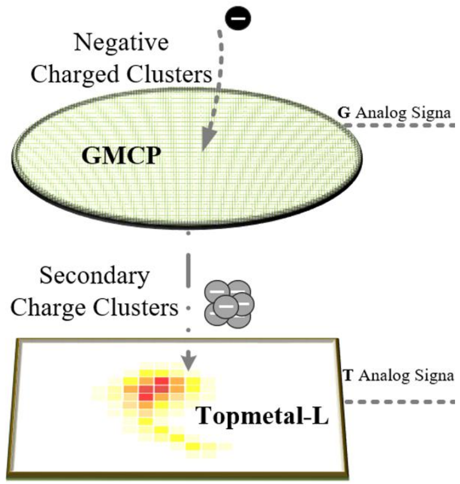

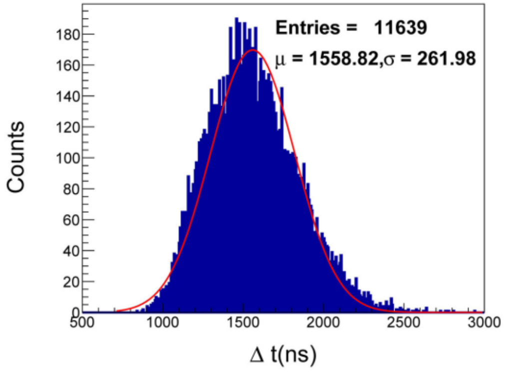

- ~262 μs time resolution

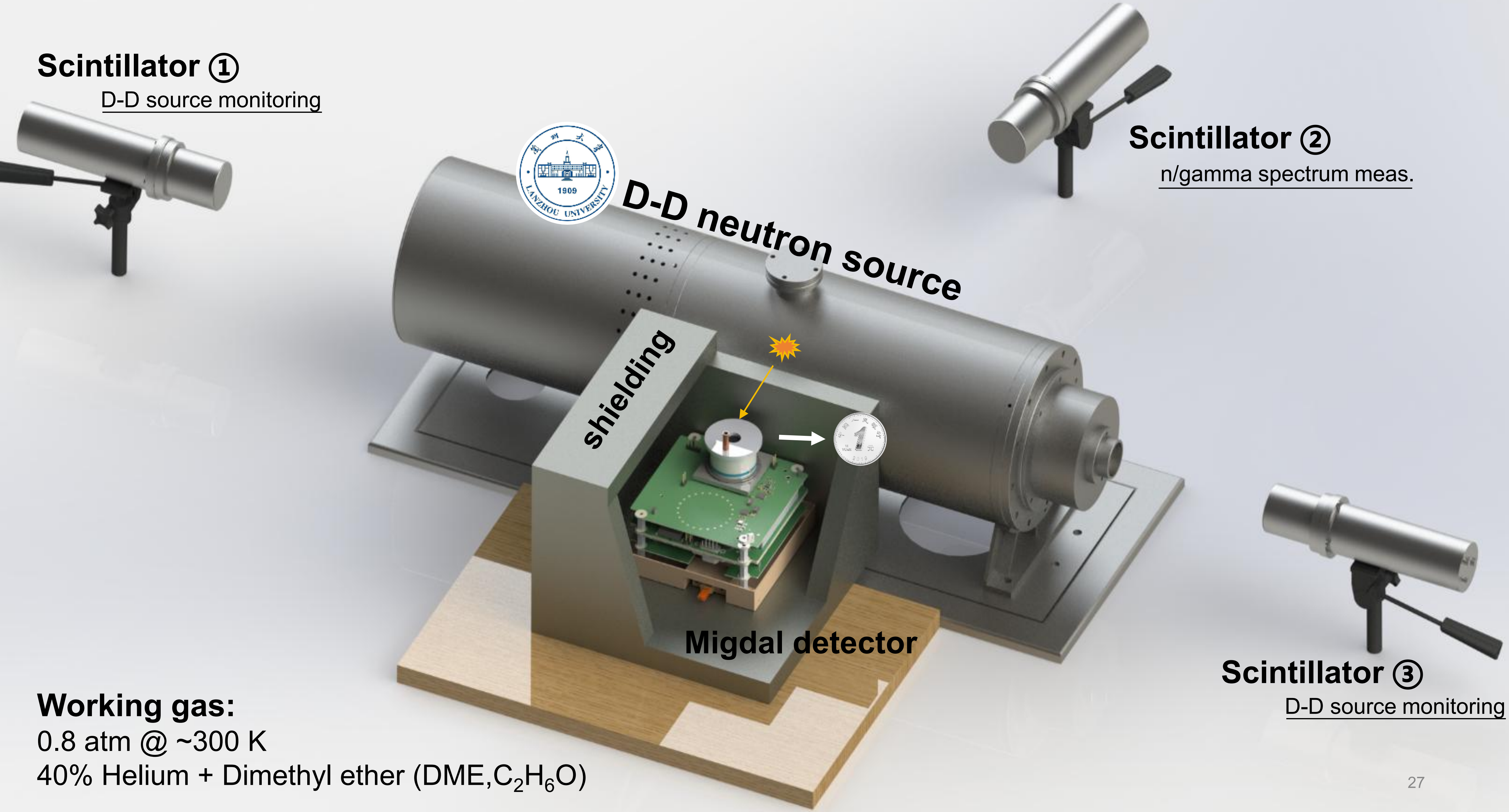

Working gas:

0.8 atm @ ~300 K

40% Helium + Dimethyl ether (DME,C_2H_6O)

事例挑选

Data → YOLO*1 preselection → NR reconstruction → ER reconstruction → Vertex cut

YOLOv8.2

Labeling

Dataset		Train	Valid
Exp	^{55}Fe	3000	1493
	D-D	2994	1354
Sim	ER	1200	301
	NR	1200	301
Total		8394	3449

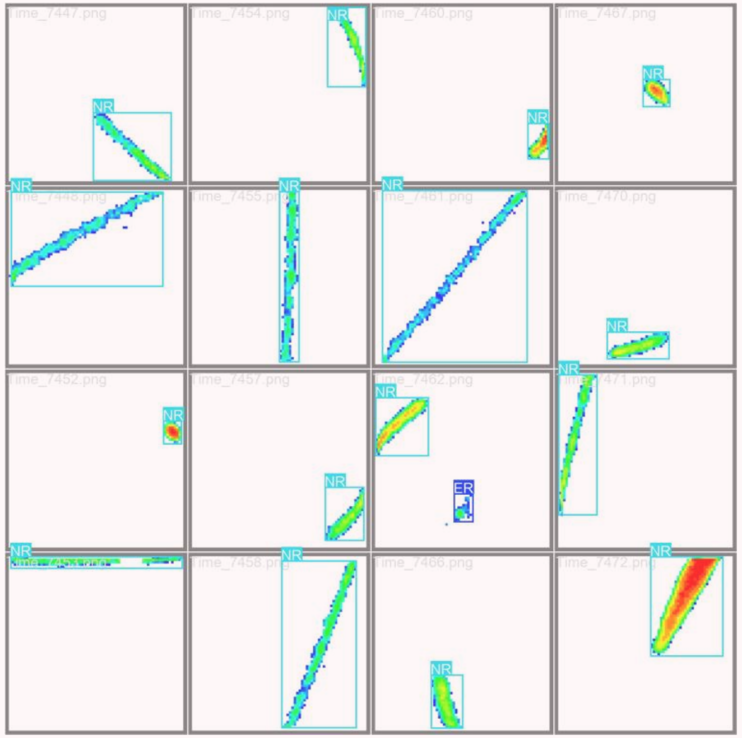

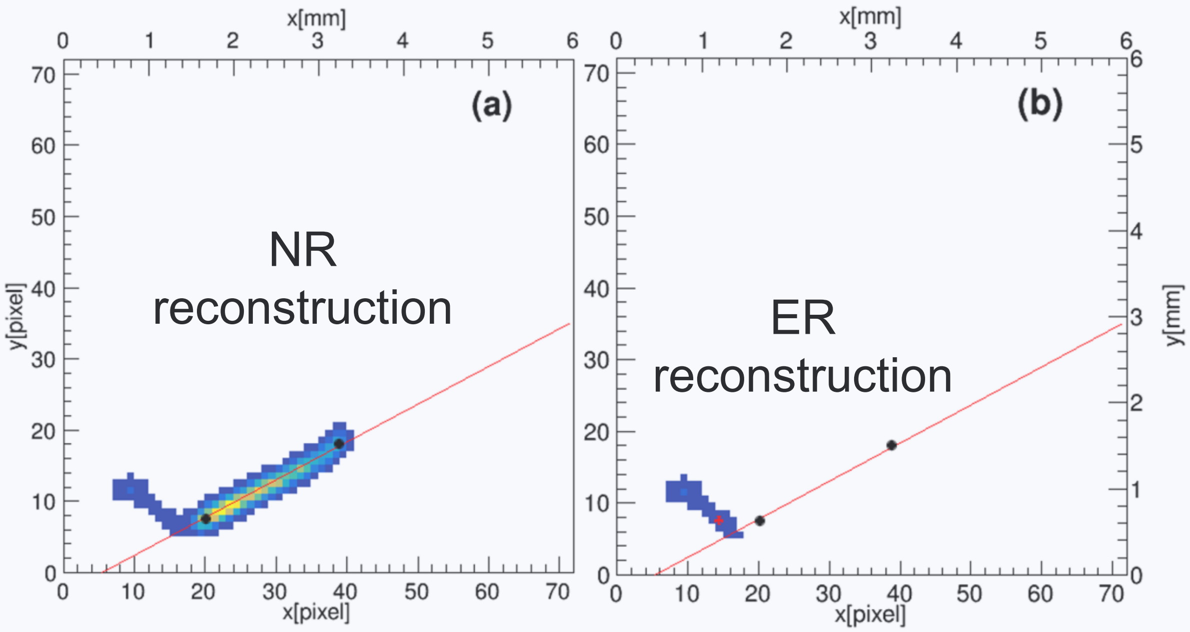

Migdal 事例

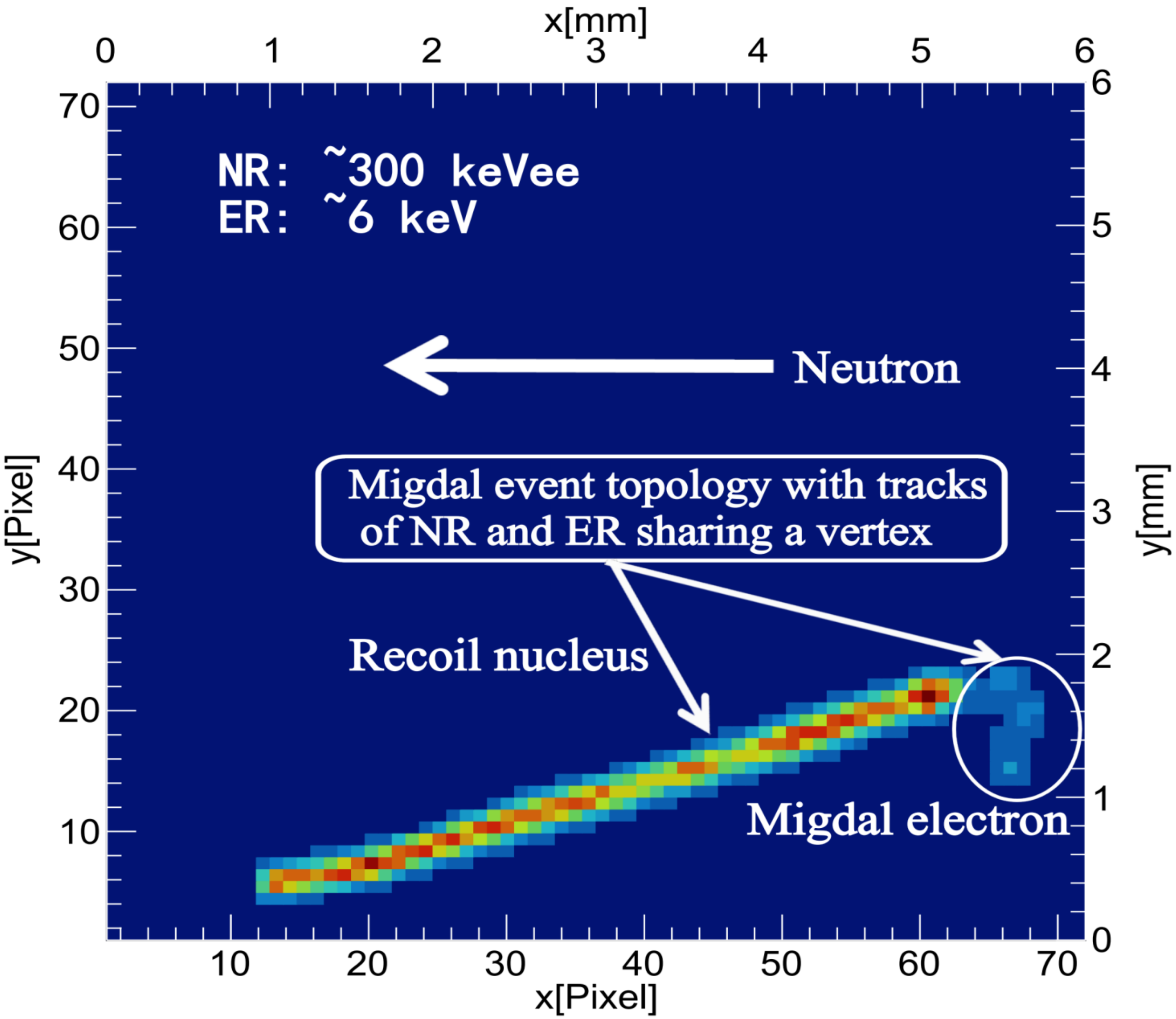
x[mm]
0 1 2 3 4 5 6
NR: ~300 keVee
ER: ~6 keV
Neutron
Migdal event topology with tracks of NR and ER sharing a vertex
Recoil nucleus
Migdal electron
y[Pixel]
70 60 50 40 30 20 10
y[mm]
6 5 4 3 2 1 0
10 20 30 40 50 60 70
x[Pixel]

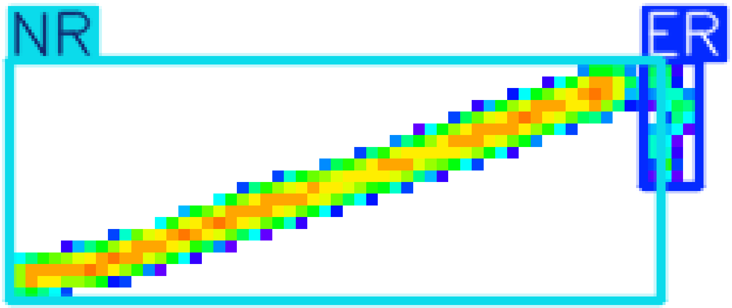
NR
ER

更多的Migdal事例！

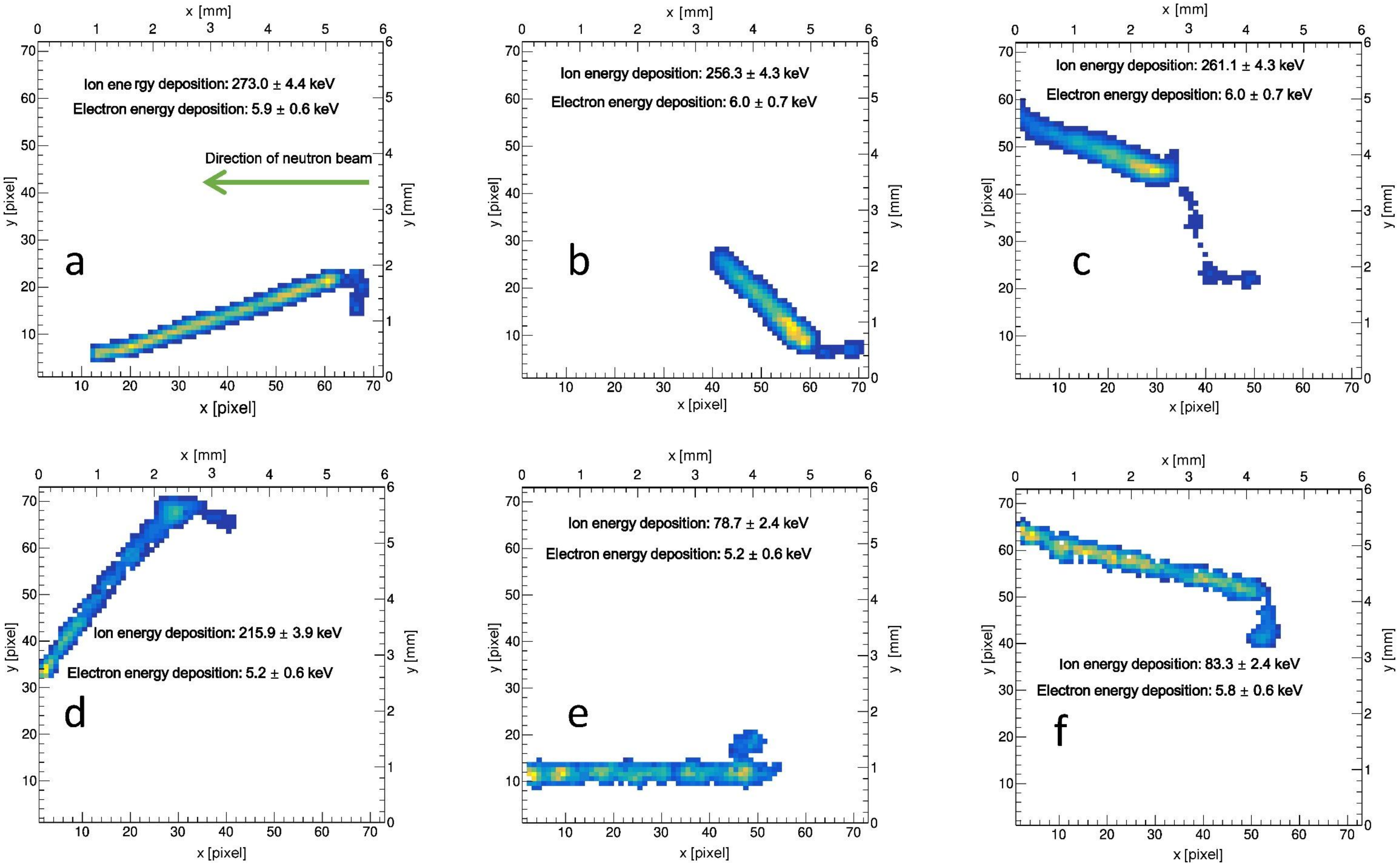

全部通过YOLO识别！

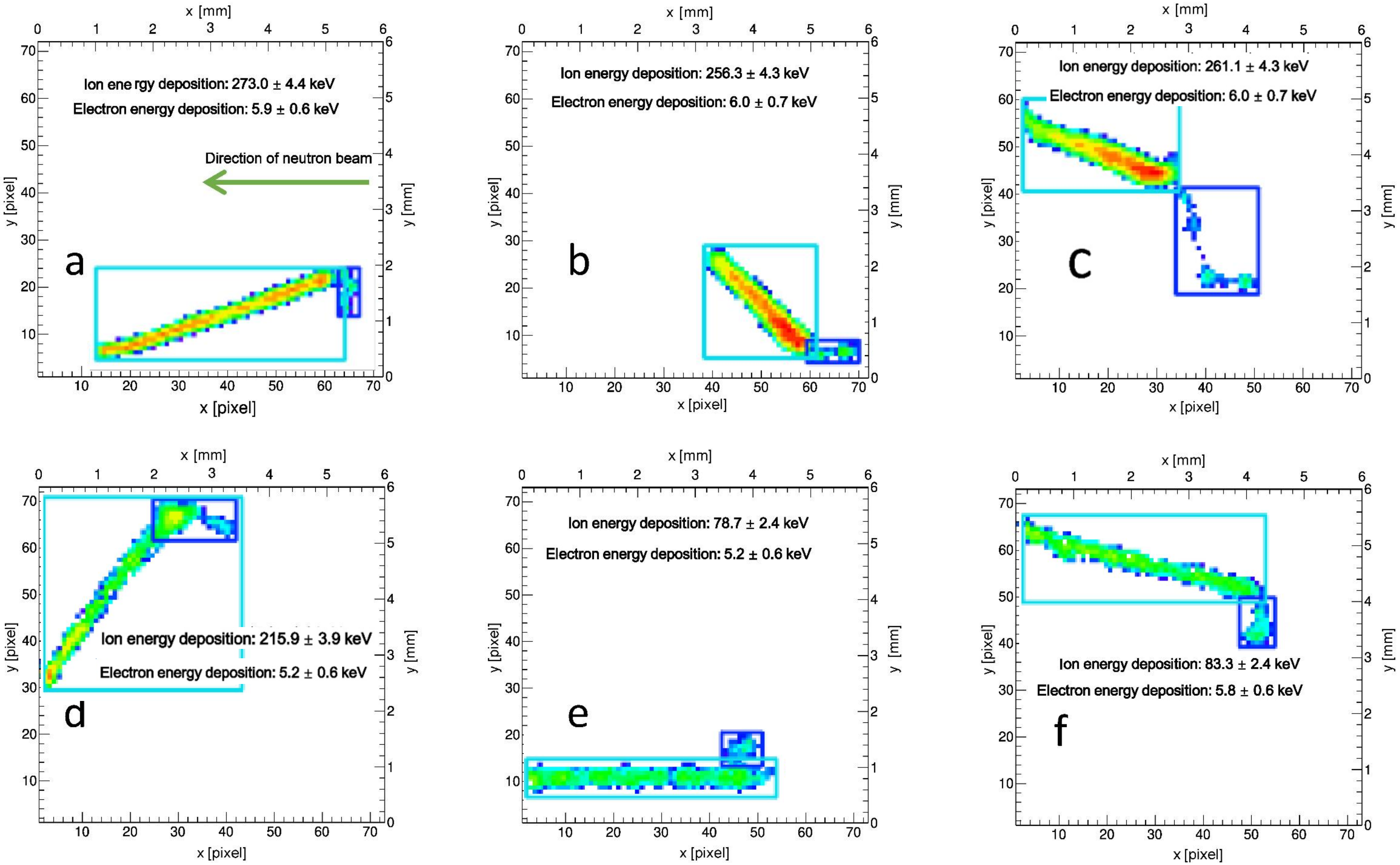

a
Ion ene rgy deposition: 273.0 ± 4.4 keV
Electron energy deposition: 5.9 ± 0.6 keV
Direction of neutron beam
b
Ion energy deposition: 256.3 ± 4.3 keV
Electron energy deposition: 6.0 ± 0.7 keV
c
Ion energy deposition: 261.1 ± 4.3 keV
Electron energy deposition: 6.0 ± 0.7 keV
d
Ion energy deposition: 215.9 ± 3.9 keV
Electron energy deposition: 5.2 ± 0.6 keV
e
Ion energy deposition: 78.7 ± 2.4 keV
Electron energy deposition: 5.2 ± 0.6 keV
f
Ion energy deposition: 83.3 ± 2.4 keV
Electron energy deposition: 5.8 ± 0.6 keV
x [mm]
y [mm]
x [pixel]
y [pixel]

电子与核子径迹

$5\ keV_{ee} < Ee < 10\ keV_{ee}, E_{nr} > 35keV_{ee}$

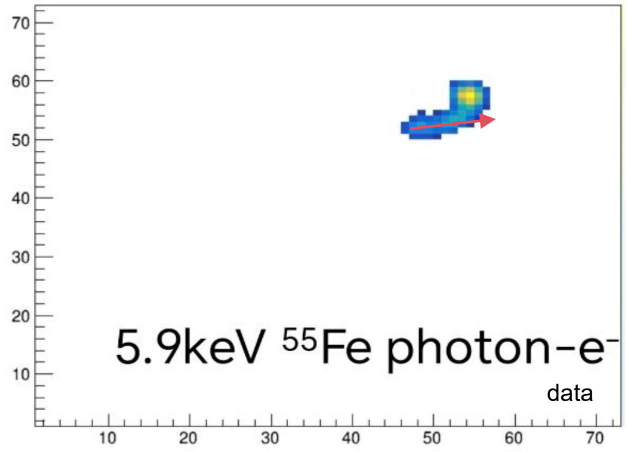

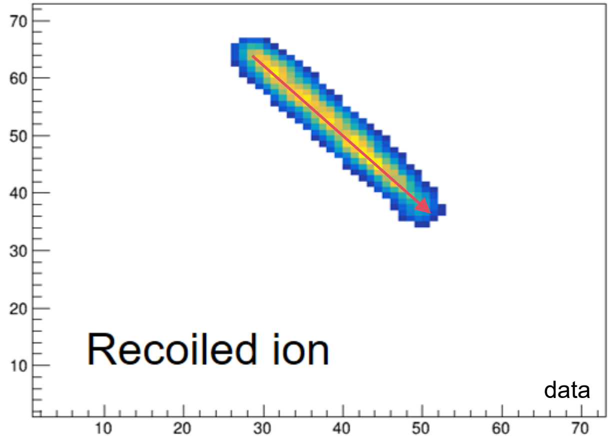

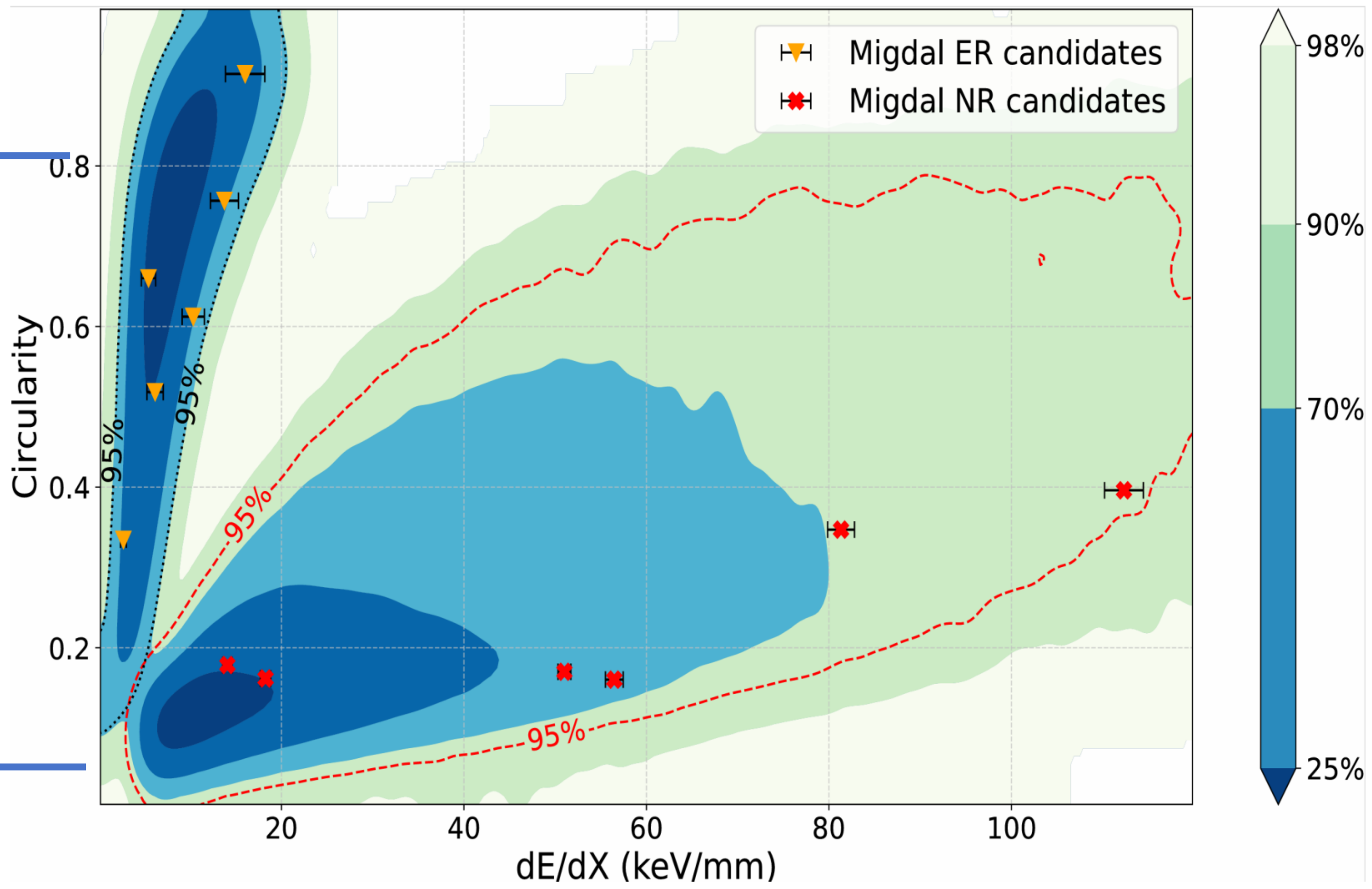

Migdal事例中的电子与^{55}Fe源的光电子样本区间一致；核反冲径迹与中子数据中核反冲控制样本一致！

本底估计

Background Component	Description	Expectation value (5 - 10 keV)	Method
Recoil induced δ ray	**δ electron near NR track origin**	**0.035±0.023(stat.)±0.0068(sys.)**	**Data driven**
Particle Induced X-ray Emission			
X-ray emission	**Photoelectron near NR track origin**	**0**	
Auger electrons	**Auger electron near NR track origin**	**0**	
Bremsstrahlung processes			
Quasi-Free Electron (QFEB)	**Photoelectron near NR track origin**	**≈ 0**	
Secondary Electron (SEB)	**Photoelectron near NR track origin**	**≈ 0**	
Atomic (AB)	**Photoelectron near NR track origin**	**≈ 0**	
Nuclear (NB)	**Photoelectron near NR track origin**	**≈ 0**	
Random track coincidences	**Photo-/Compton electron near NR track**	**0.180±0.022(stat.)±0.042(sys.)**	**Data driven**
Muon induced δ ray	**δ electron near NR track origin**	**0.013**	**MC+Data**
Gas radioactivity			
Trace contaminants	**Electron from decay near NR track origin**	**0.001±0.00087(sys.)**	**Data driven**
Neutron activation	**Electron from decay near NR track origin**	**≈ 0**	
Secondary nuclear recoil fork	**NR track fork near track origin**	**≈ 0**	
Total background		**0.229±0.032(stat.)±0.043(sys.)**	

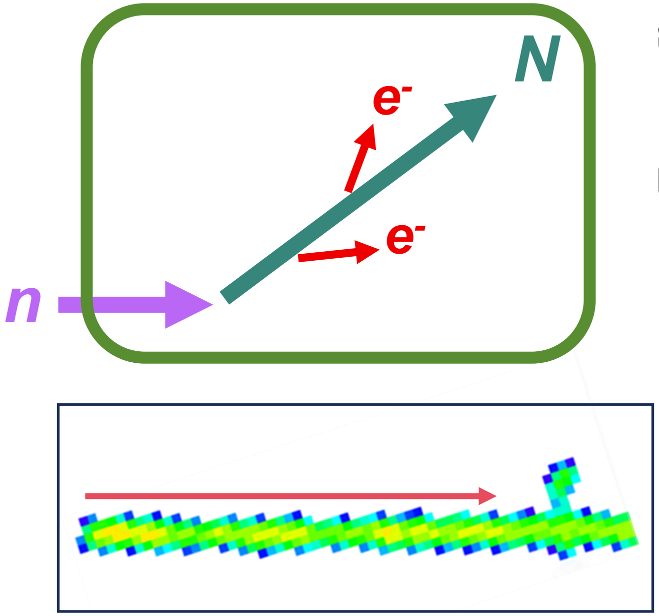

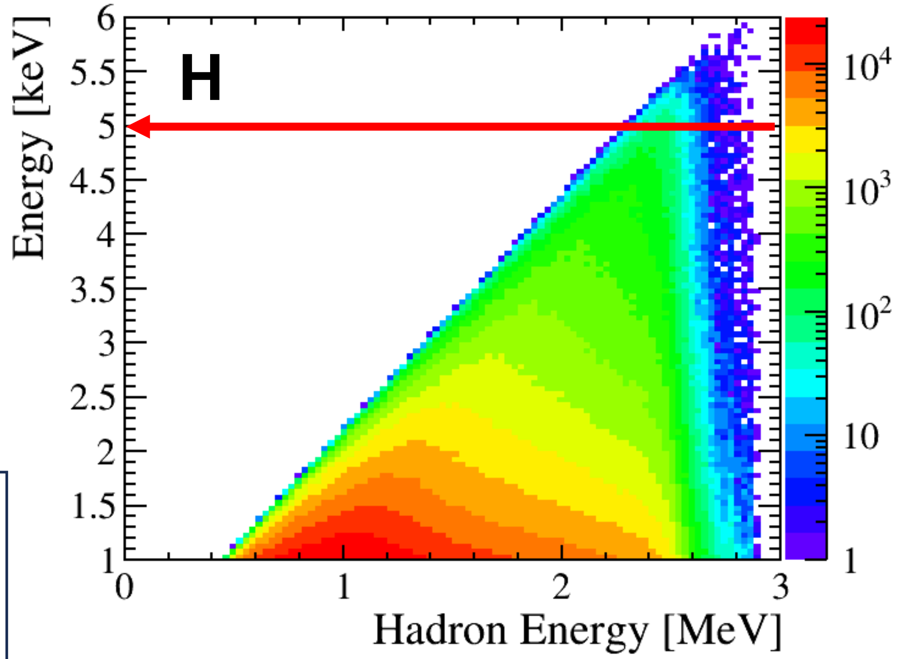

Only H has the **δ electron >** 5 keV.

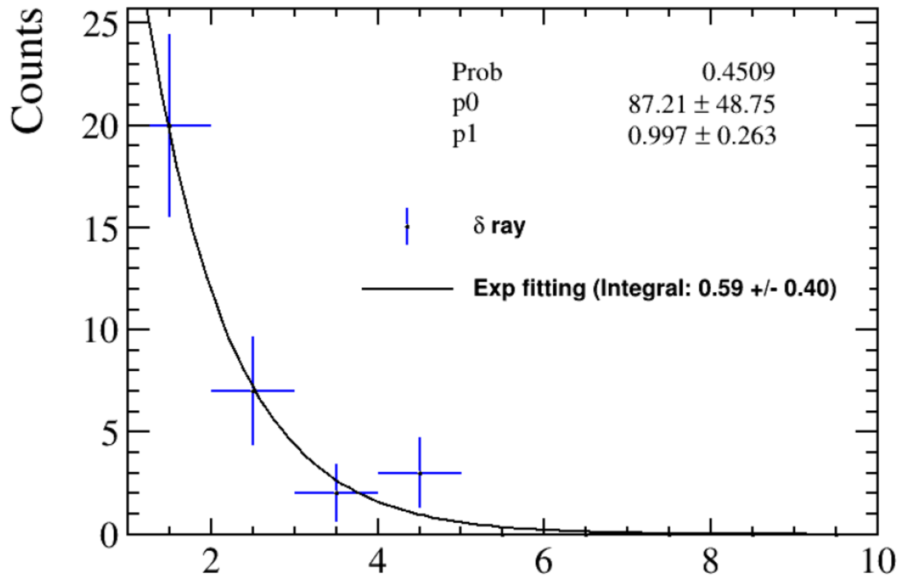

No δ above 5 keV were found.

Estimate by extrapolating from the exponential fit

- Consider the selection efficiency for δ-electrons.
- **Finally get: 0.035±0.023(stat.)**

2. Radom track conincidence

Method 1: n/γ spectrum measured by LS + GEANT4

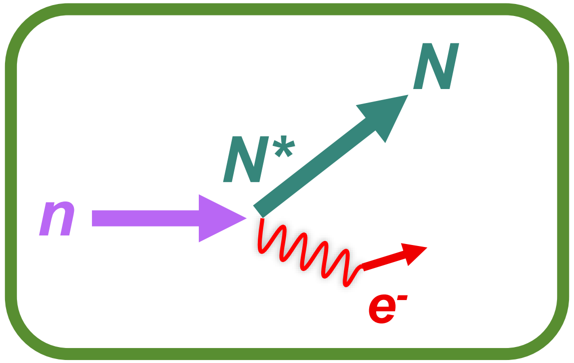

I

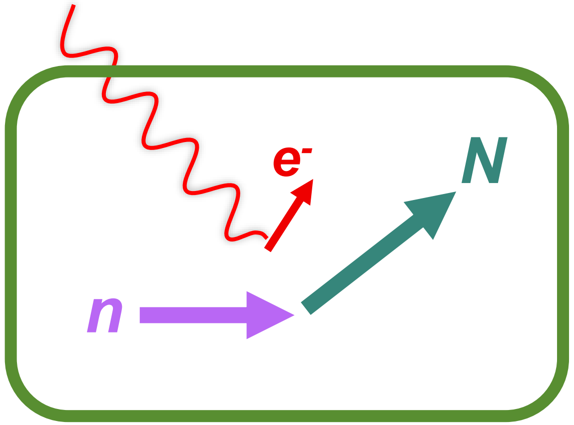

II

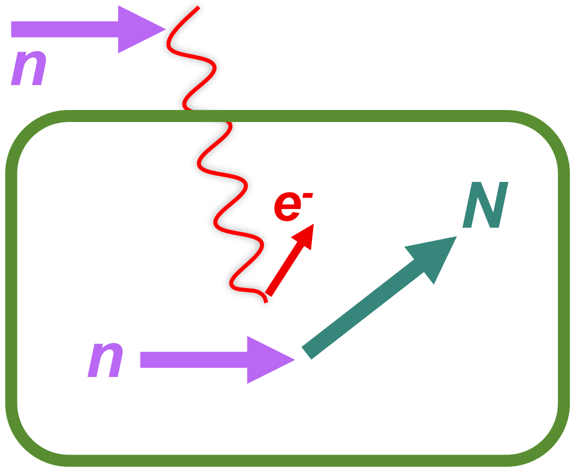

III

	NR	Compton e-	photonEle
I	1	4.32×10^{-5}	1.06×10^{-5}
II	1	6.06×10^{-6}	$\sim 3.63 \times 10^{-8}$
III	1	3.11×10^{-6}	7.15×10^{-7}

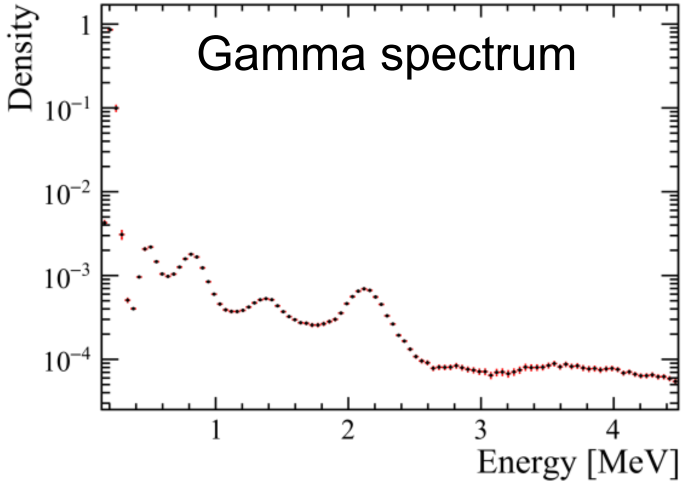

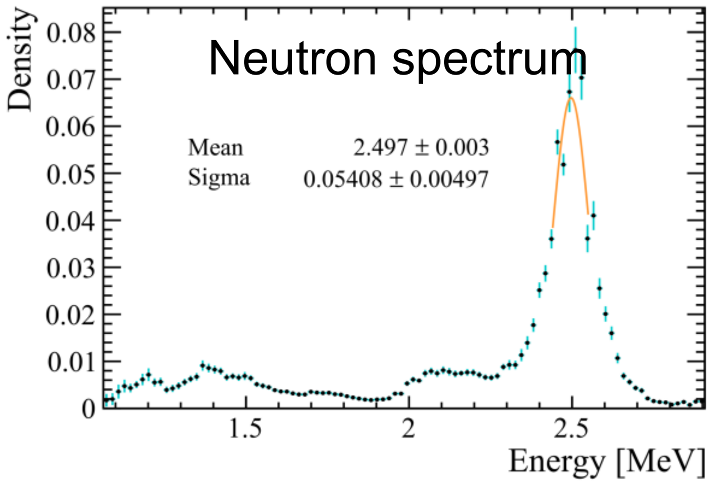

- **The expected background contribution of the 3 components in total is: 0.16±0.01(stat.)**

Radom track conincidence

- **Method 2: Estimated from Data**
  - Get the number of electron tracks within the 5-10 keV energy range that appear in the same frame as the nucleon tracks.
  - Considering the accidental coincidence of NR and ER with a vertex selection efficiency,
  - the final expected background value is **0.180±0.022(stat.)±0.042(sys.)**

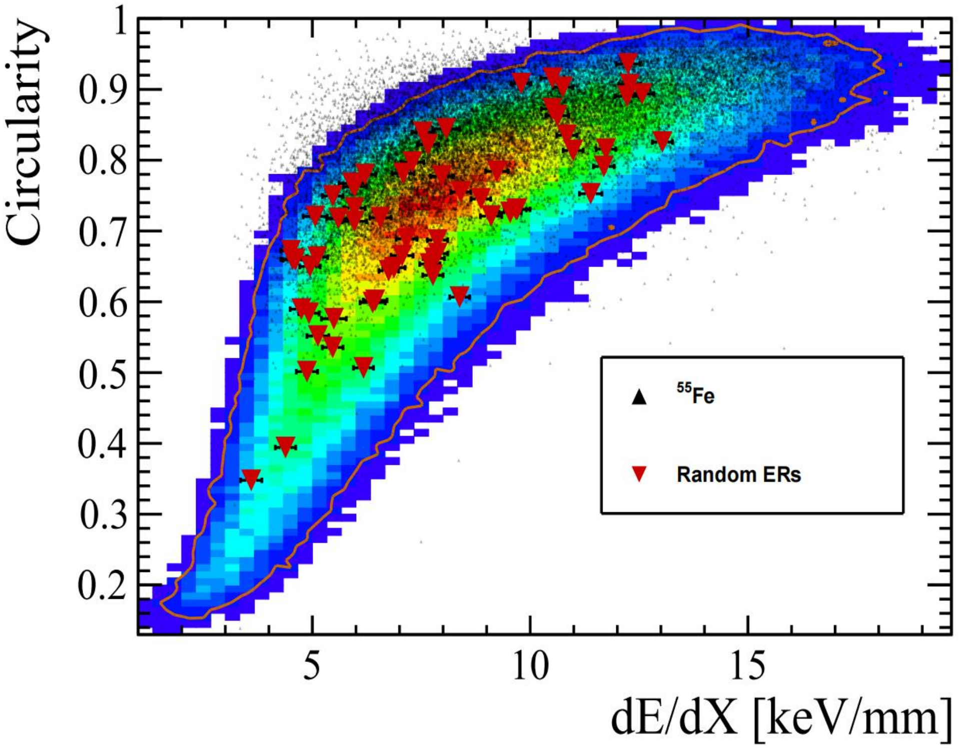

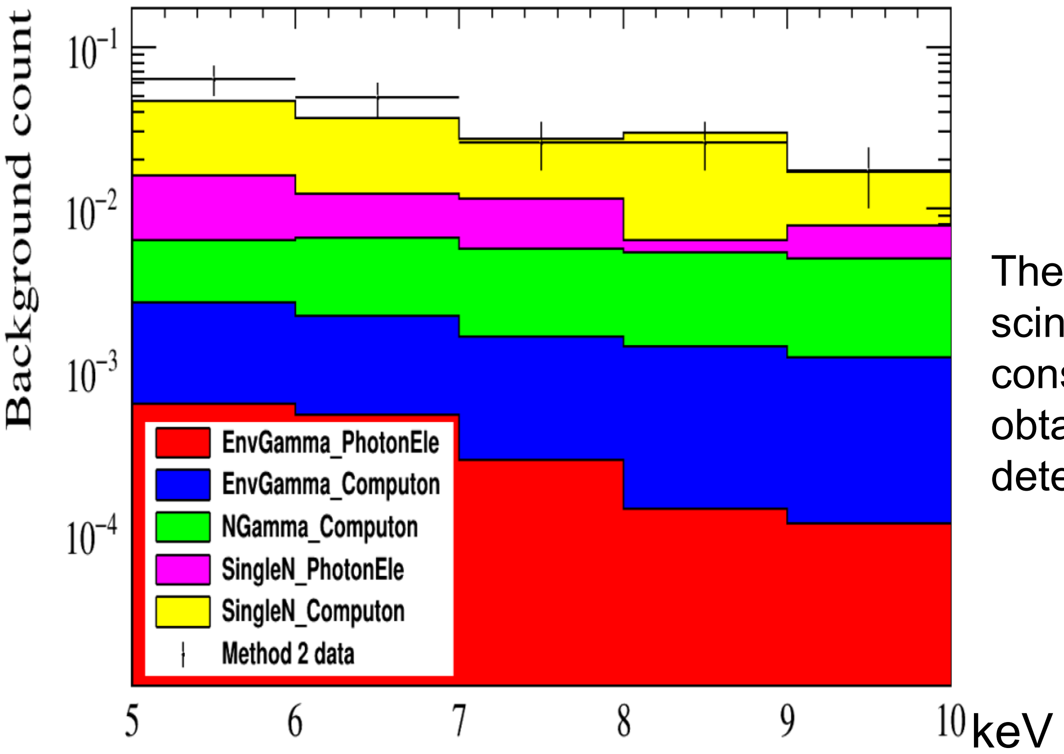

The results from the liquid scintillation + GEANT4 are consistent with the data obtained from the Migdal detector.

Cross section ratio calculation

- Probability: $$P_{\text{Migdal}}(5\text{keV}<\text{ER}<10\text{keV},\ \text{NR}>35\text{keVee})=\frac{\left(\frac{n_{\text{obs}}^{\text{ER}}-n_{\text{obs}}^{\text{bg}}}{\varepsilon_{\text{acc}}\varepsilon_{\text{NR}}\varepsilon_{\text{ER}}}\right)}{\left(\frac{n_{\text{tot}}^{\text{NR}}}{\varepsilon_{\text{acc}}\varepsilon_{\text{NR}}}\right)}=\frac{(n_{\text{obs}}^{\text{ER}}-n_{\text{obs}}^{\text{bg}})}{\varepsilon_{\text{ER}}n_{\text{tot}}^{\text{NR}}}$$
- Parameters:

	Efficiency/Count	Statistical Error	Systematic Error
Efficiency ε_{ER}	14.4% 29%(YOLO)*49%(vertx rec)	±0.1%	±1.9%
$n_{\text{tot}}^{\text{NR}}$	8.17×10^5	±903	±35880
$n_{\text{obs}}^{\text{ER}}$	6		
$n_{\text{obs}}^{\text{bg}}$	0.229	±0.032	±0.043

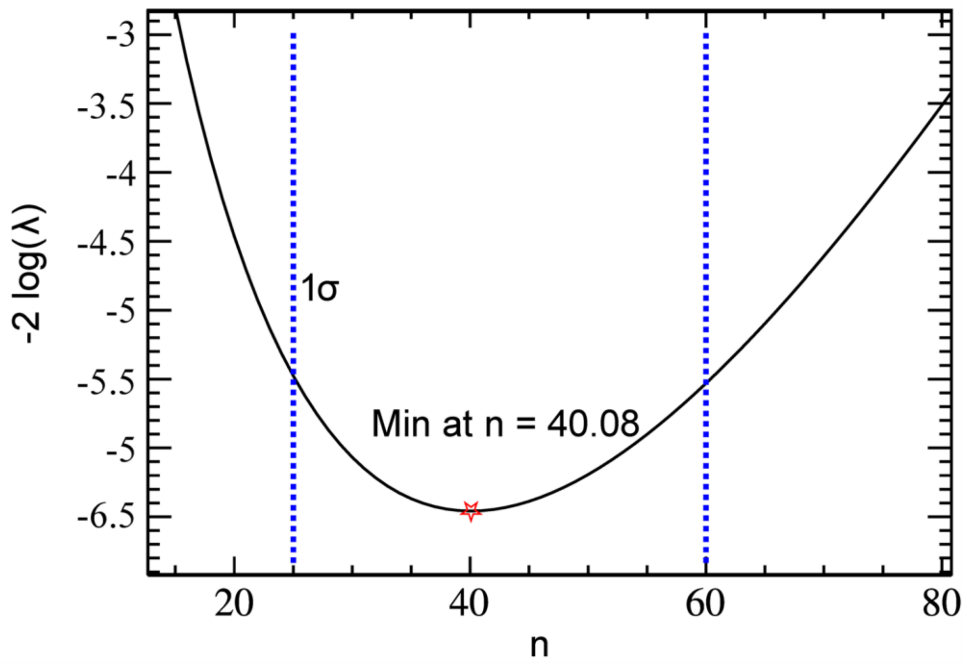

- upper/lower bounds: $$\Delta P_{\pm}=\sqrt{\left(\frac{n_{min}-n_{ul/ll}}{n_{min}}\right)^2+\left(\frac{n_{\text{tot}\,error}^{\text{NR}}}{n_{\text{tot}}^{\text{NR}}}\right)^2}\cdot\frac{n_{min}}{n_{\text{tot}}^{\text{NR}}}$$

Result: $4.9^{+2.6}_{-1.9}\times 10^{-5}$

Theory: 3.9×10^{-5}

The total transition probability

$$\sum_{nl} \frac{dp^i(nl \to E_e)}{dE_e}$$

初态为 (n,l) 的电子跃迁到具有 E_e 能量末态的几率.

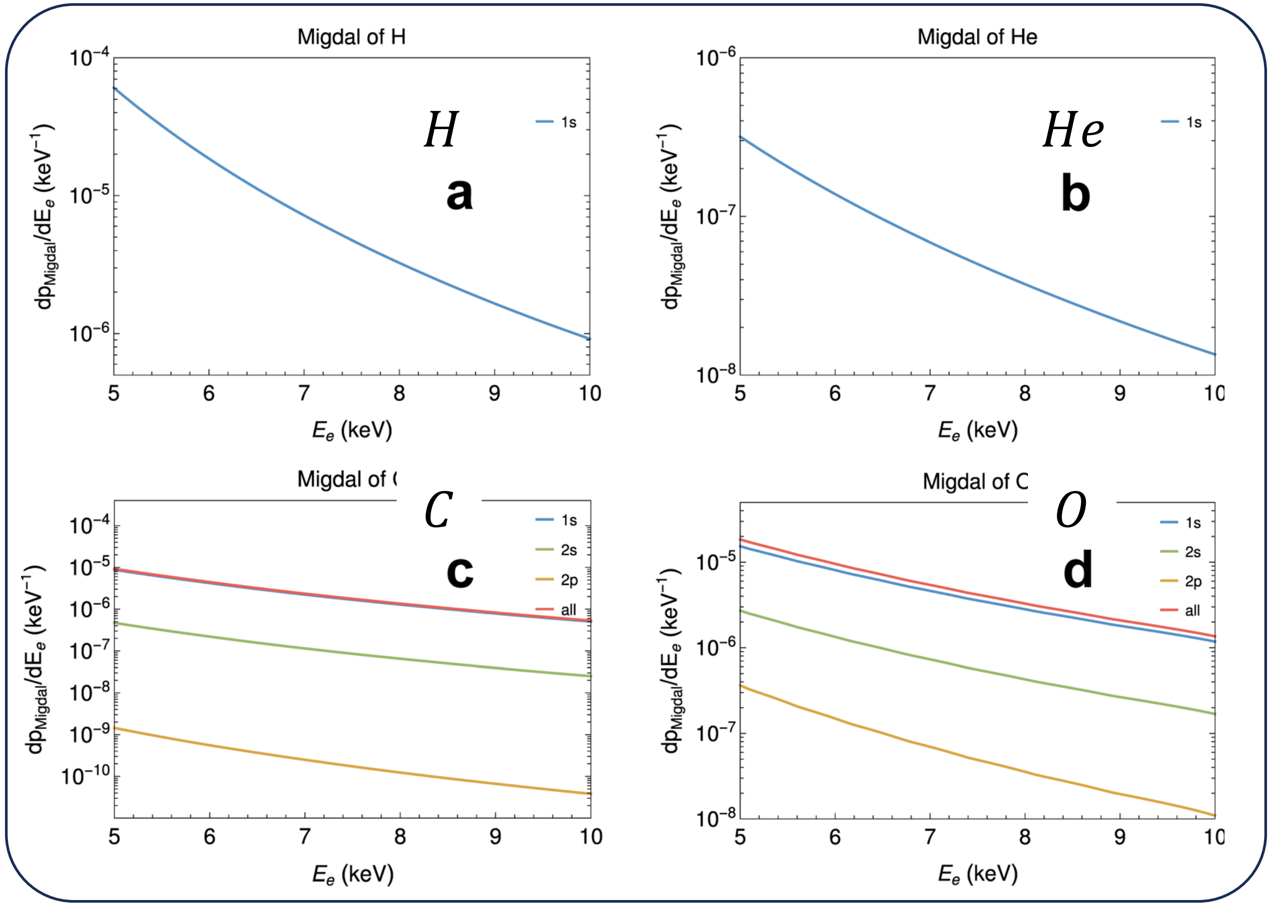

每种元素的跃迁几率

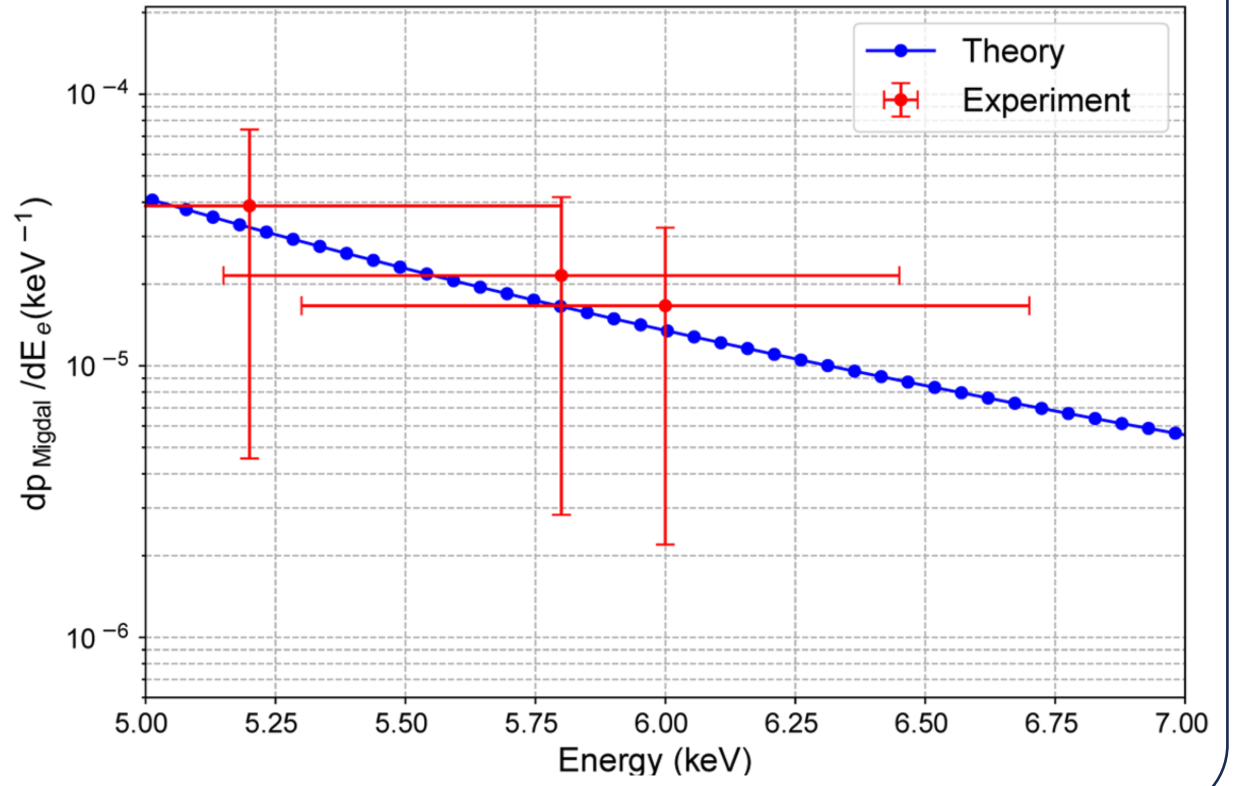

总跃迁几率

Upgrade in progress

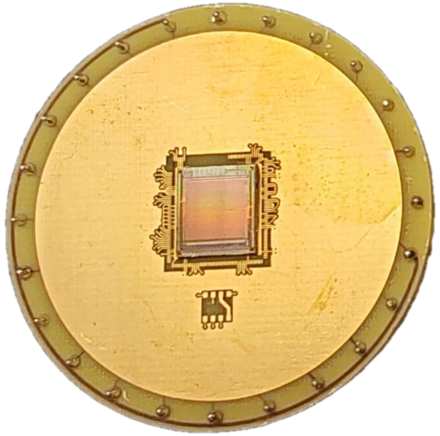

Topmetal-II

Topmetal-L

	Topmetal-II^{-}	Topmetal-L
Chip size [mm^2]	8×9	17×24
Active area [mm^2]	6×6	16.02×23.04
Pixel array	72×72	356×512
Pixel density [pixels/mm^2]	145	494
Power density [W/cm^2]	2.778	0.195
Pixel gain [μV/e^{-}]	-	76.04
ENC [e^{-}]	13.9	22.8
Readout mode	Rolling Shutter	Rolling Shutter / Sentinel
Time cost	2.6 ms/frame	0.73 ms/frame @ Sentinel

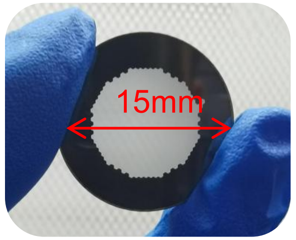

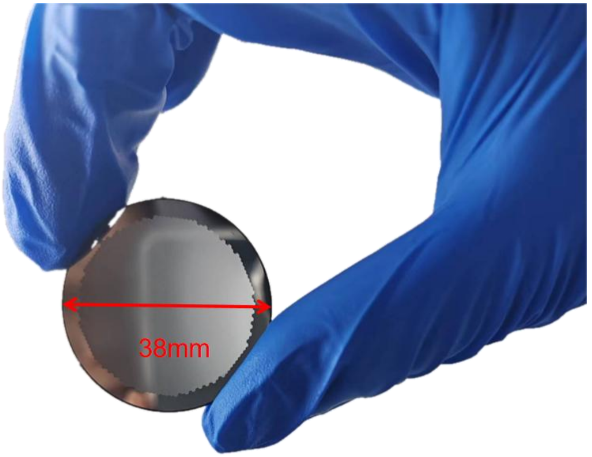

Larger GMCP

- 6x6 mm, 83 um in pitch -> 2.3x1.5 cm, 45 um in pitch
- Fresh time: 2.6 ms/Frame -> 0.7 ms/Frame
- Readout logic: Rolling Shutter -> Sensitive area

Upgrade in progress

Sensitive area readout:

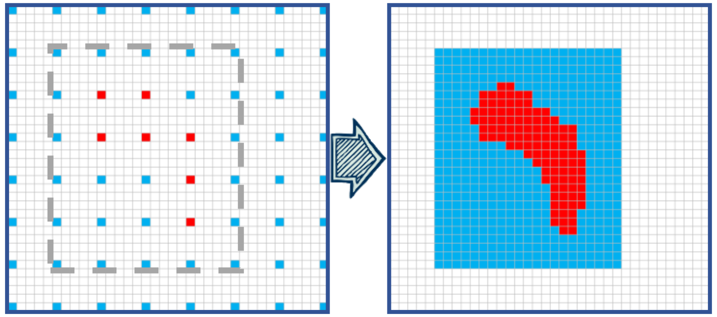

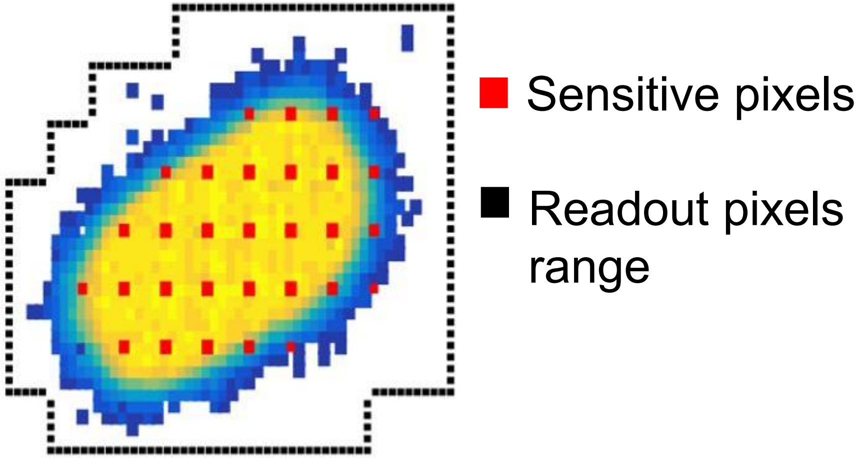

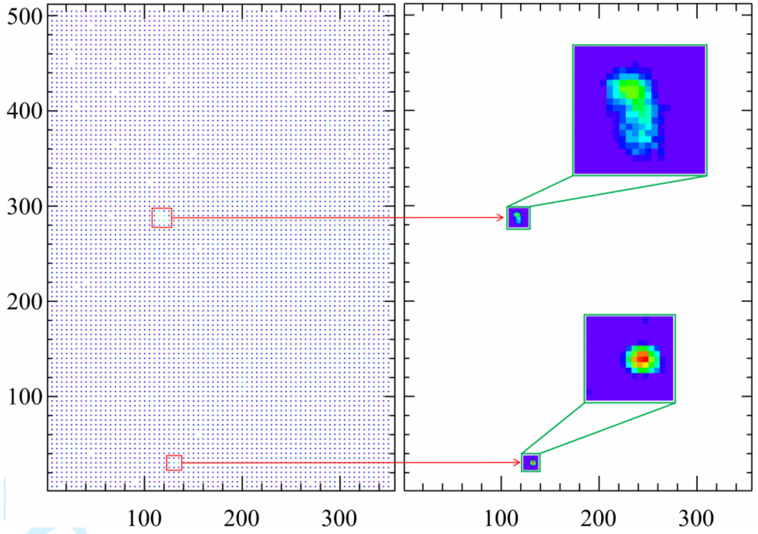

arXiv:2511.15130

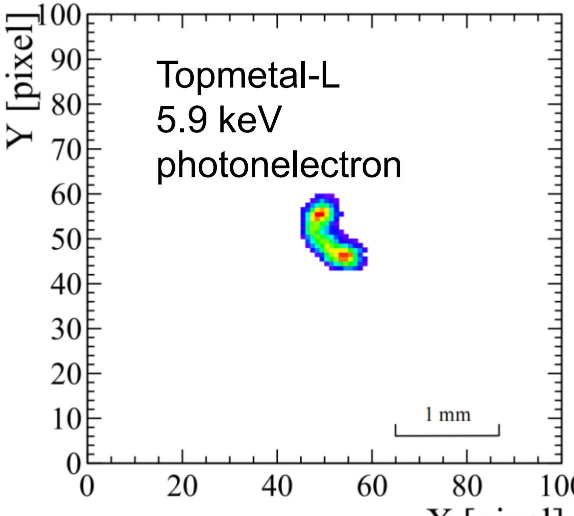

arXiv:2511.09863

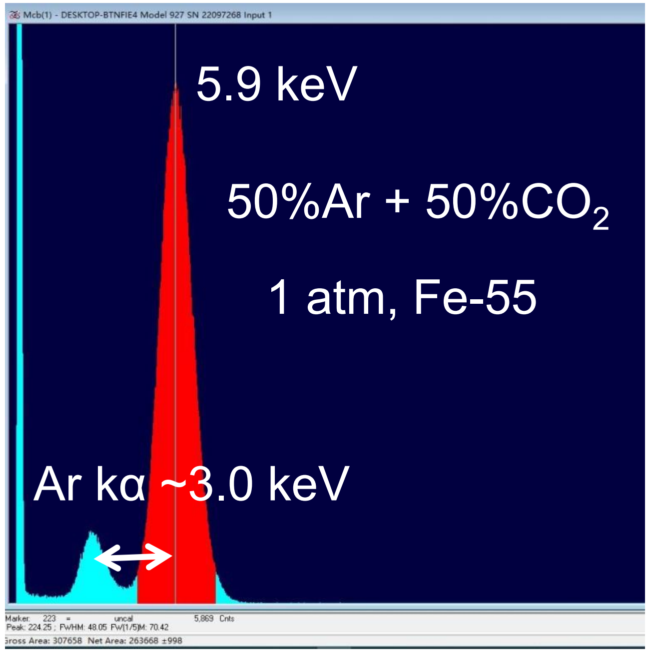

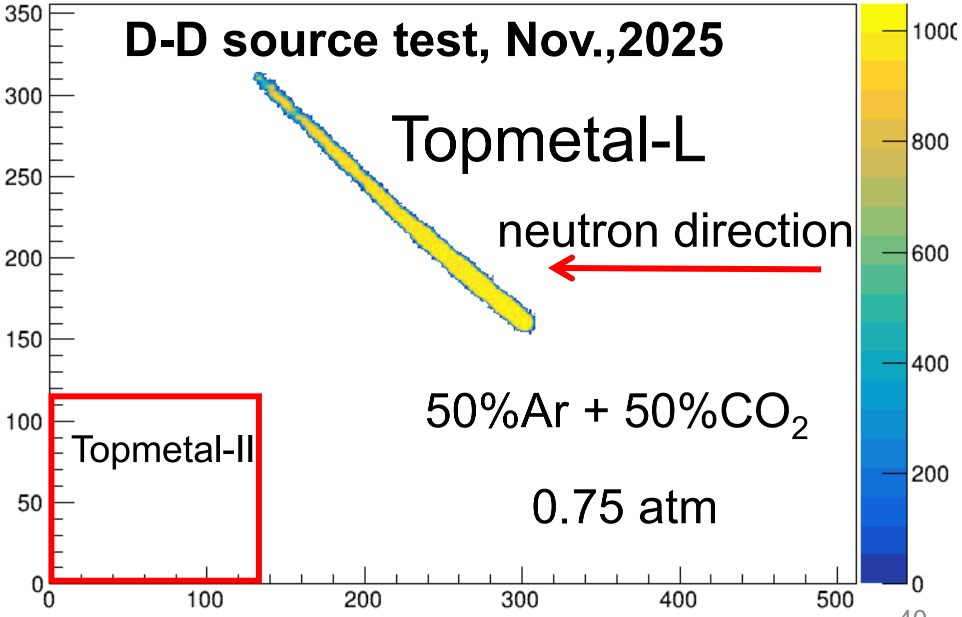

- The Migdal effect plays a very important role in light dark matter research.
- The MARVEL experiment is dedicated to the direct detection of the Migdal effect.
- The ratio of the Migdal to the nuclear recoil cross-section to be $4.9^{+2.6}_{-1.9} \times 10^{-5}$, where nuclear recoils exceed 35 keVee and electron recoils span 5-10 keV.
- Detector upgrade is in progress.

Thanks for your attention!